Preparation of Open-Shell Donors and Intramolecular Exchange Interaction of Their One-Electron Oxidation States

（開殻ドナー分子の合成とその一電子酸化状態における分子内交換相互作用）

瀧 井　功 児

December, 1994

(1)

Preparation of Open-Shell Donors and Intramolecular Exchange Interaction of Their One-Electron Oxidation States

A Thesis
Submitted to
the University of Tokyo
in Fulfillment of the Requirement
for the Degree
of
Doctor (Science)

by
Reiji Kumai

December, 1994

This thesis was written principally based on the papers already published or to be published as listed below.

[1] Structure and Physical Properties of Two Perchlorate Salts Deriver from a Novel Twin Donor. Bis(4',5'-ethylenedithio-5-methylthiotetrathia-fulvalenyl-4-thio)methane
A. Izuoka, R. Kumai, and T. Sugawara, *Chem. Lett.*, **1992**, 285-288.

[2] Intramolecular Exchange Interaction in a Novel Cross-Conjugated Spin System Composed of π-Ion Radical and Nitronyl Nitroxide
Reiji Kumai, Michio M. Matsushita, Akira Izuoka, and Tadashi Sugawara, *J. Am. Chem. Soc.*, **116**, 4523 (1994).

[3] Ground State Triplet Cation Biradicals Based on Non-Degenerated Singly Occupied Molecular Orbitals
Reiji Kumai, Akira Izuoka, Tadashi Sugawara, to be submitted.

[4] Ground State Electron Spin Multiplicity of Cation Biradical of Open-Shell Donor. Exchange Interaction between Two Types of Non-Degenerated SOMOs.
Reiji Kumai, Akira Izuoka, Tadashi Sugawara, to be submitted.

Acknowledgment

This thesis work was carried out under the guidance of Professor Tadashi Sugawara. The author would like to thank him for his continuous interest in this work and many valuable discussions and useful advice and encouragement throughout the course of the present work.

The author wished to thank Dr. Akira Izuoka for his collaboration and useful discussions and technical assistance.

Thanks are also to Profs. K. Itoh, T. Takui and Y. Teki in Osaka City Univ. for offering an ESR simulation program.

The author wishes to thank Mr. Michio M. Matsushita and Miss Hiromi Sakurai and Miss Kumiko Ozawa for their collaboration.

The author wishes to express his gratitude to all the members of this laboratory.

December, 1994

Contents

1. Introduction

In general, organic materials are diamagnets. This is because they consist of organic molecules with a close-shell electronic structure. Free radical is an exception, having an open-shell electronic structure. When stable radicals are assembled, they behave as paramagnets, sometimes exhibiting a very weak antiferromagnetic interaction. Recently organic ferromagnets are discovered[1]. Now the long- standing concept for organic materials should be renewed. However, phase transition temperatures to the ferromagnetic phase, so far reported, are extremely low (< 1K or ca. 1K). Therefore it is hard to elucidate the accurate mechanism of spin ordering in these organic ferromagnets. Besides, development of devices based on organic ferromagnetism is impractical at the present stage, because of the extremely low Tc. It is time to construct organic ferromagnets with high Tc, and to investigate the mechanism of spin ordering based on the well-defined crystal structure.

When inorganic compounds are looked around, ferromagnets are frequently encountered, for instance 3*d* metals, rare-earth metals, ferromagnetic diluted alloys, etc[2]. In these compounds, itinerant electrons play an important role in aligning electron spins. In 4*f* metals, for example, 4*f* electron spins are in parallel based on Hund rule. When itinerant 5*s* electrons come to the lattice point, they suffer from the effective exchange

interaction with localized 4*f* spins. Thus probability of finding up- or down-spin of the itinerant electron is modulated based on the spin polarization caused by the effective exchange interaction with the localized 4*f* spins. Since such a spin polarization is transmitted as a damping oscillation to the next lattice point at which 4*f* spins await, all the 4*f* spins align to the same direction, if the phase of the spin polarization of the itinerant electron matches at each lattice point. As a result, ferromagnetic spin ordering in 4*f* metals is achieved. This mechanism of spin ordering is known as RKKY theory[3], and the theory is applied successfully to rationalize the ferromagnetic spin ordering in 4*f* metals or ferromagnetic diluted alloys (Figure I-1).

$La_xSr_{1-x}MO_3$ (M=Mn, Co)[4] is a recent example in which ferromagnetic spin ordering can be explained by the similar mechanism. The ferromagnetic interaction, which is called as "double exchange"[5], exists between localized spins (t_{2g} orbital electrons) and itinerant electrons (e_g orbital electrons). As a result, all spins located in 3*d* orbitals align to the same direction through itinerant electrons (Figure I-2). In 3*d* metals, however, itineracy of 3*d* electrons makes the situation more complex. Therefore RKKY theory can not be applied in this case.

Looking upon the mechanism of spin alignment of inorganic compounds with itinerant electrons, it occurs to one's mind that one of the strategies of obtaining high Tc ferromagnets is to construct an organic ferromagnetic

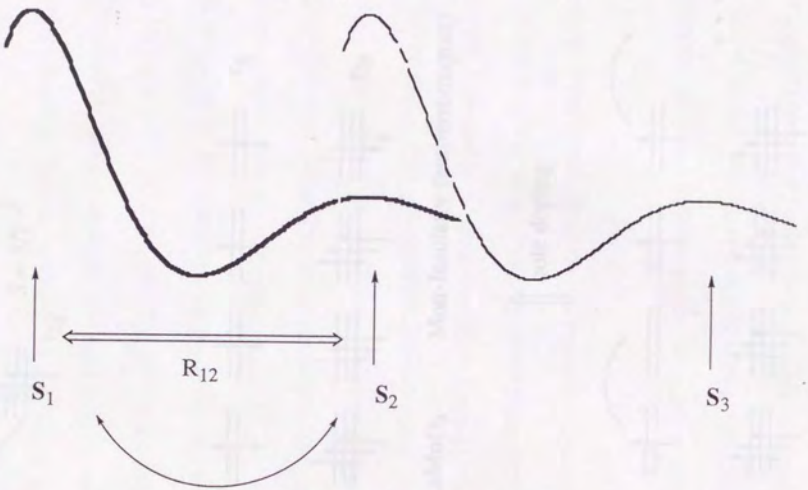

Figure I-1 Spin alignment mechanism based on RKKY theory.

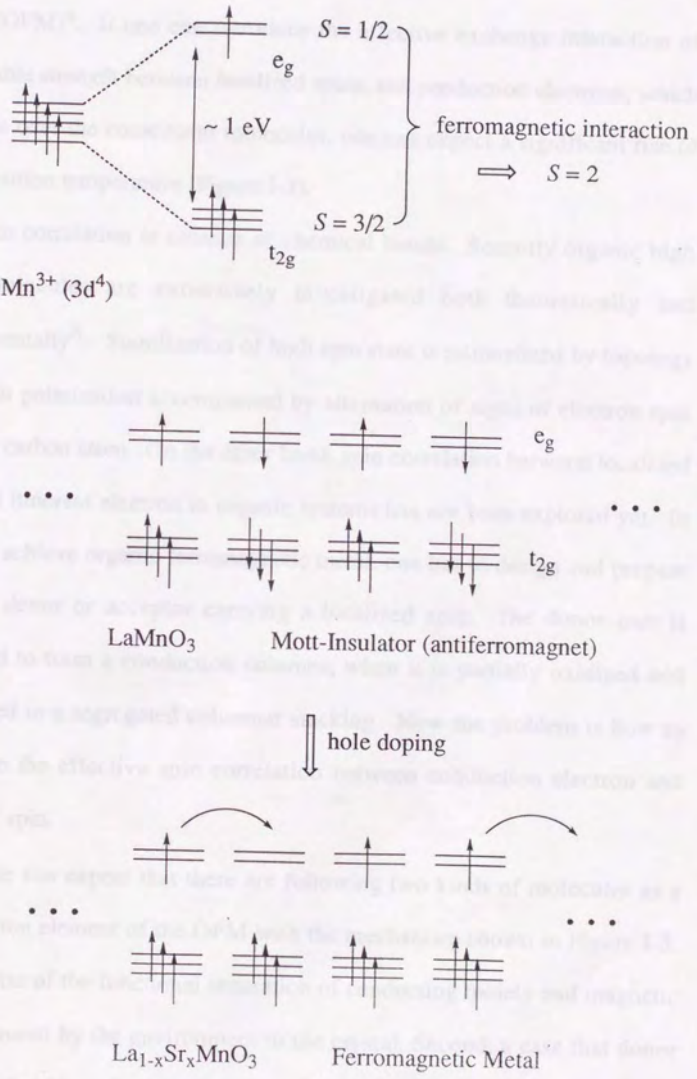

Figure I-2. Spin alinment mechanism of $La_{1-x}Sr_xMnO_3$.

metal (OFM)[6]. If one can introduce the effective exchange interaction of reasonable strength between localized spins, and conduction electrons, which itinerate over the constituent molecules, one can expect a significant rise of the transition temperature (Figure I-3).

Spin correlation is essence of chemical bonds. Recently organic high spin molecules are extensively investigated both theoretically and experimentally[7]. Stabilization of high spin state is rationalized by topology of π-spin polarization accompanied by alternation of signs of electron spin on each carbon atom. On the other hand, spin correlation between localized spin and itinerant electron in organic systems has not been explored yet. In order to achieve organic ferromagnetic metal, one has to design and prepare a novel donor or acceptor carrying a localized spin. The donor part is supposed to form a conduction columns, when it is partially oxidized and assembled in a segregated columnar stacking. Now the problem is how to introduce the effective spin correlation between conduction electron and localized spin.

One can expect that there are following two kinds of molecules as a composition element of the OFM with the mechanism shown in Figure I-3. First, a case of the functional separation of conducting moiety and magnetic moiety caused by the environment in the crystal. Second, a case that donor moiety and stable radical moiety are distinguished beforehand.

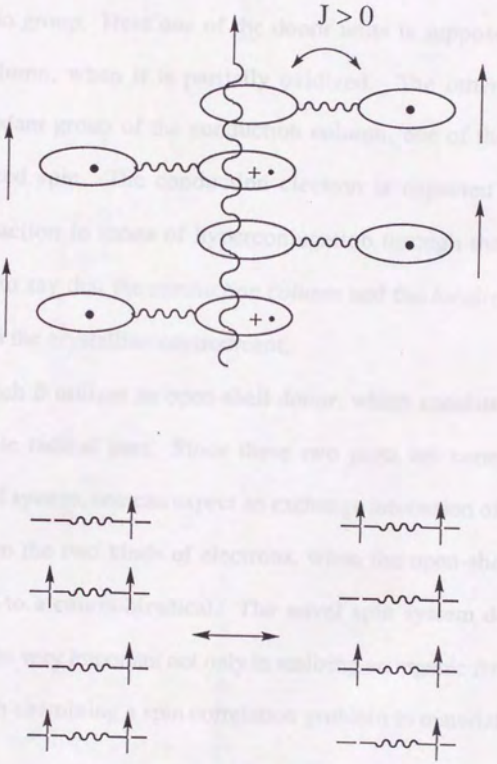

Figure I-3. Schematic structure of OFM

In this thesis, the author describes two approaches (Approach *A* and *B*) to construct organic ferromagnetic metals (Figure I-4). The approach *A* utilizes a twin donor, which has two equivalent donor units connected with a methylenedithio group. Here one of the donor units is supposed to form a conduction column, when it is partially oxidized. The other donor part becomes a pendant group of the conduction column, one of the every two holds a localized spin. The conduction electron is expected to have an exchange interaction in terms of hyperconjugation through the methylene group. That is to say that the *conduction column* and the *localized spin*, are discriminated in the crystalline environment.

The approach *B* utilizes an open-shell donor, which consists of a donor part and a stable radical part. Since these two parts are connected by a cross-conjugated system, one can expect an exchange interaction of reasonable strength between the two kinds of electrons, when the open-shell donor is singly oxidized to a cation-biradical. The novel spin system documented here is found to be very important not only in realizing an organic ferromagnetic metal, but also in examining a spin correlation problem in materials science.

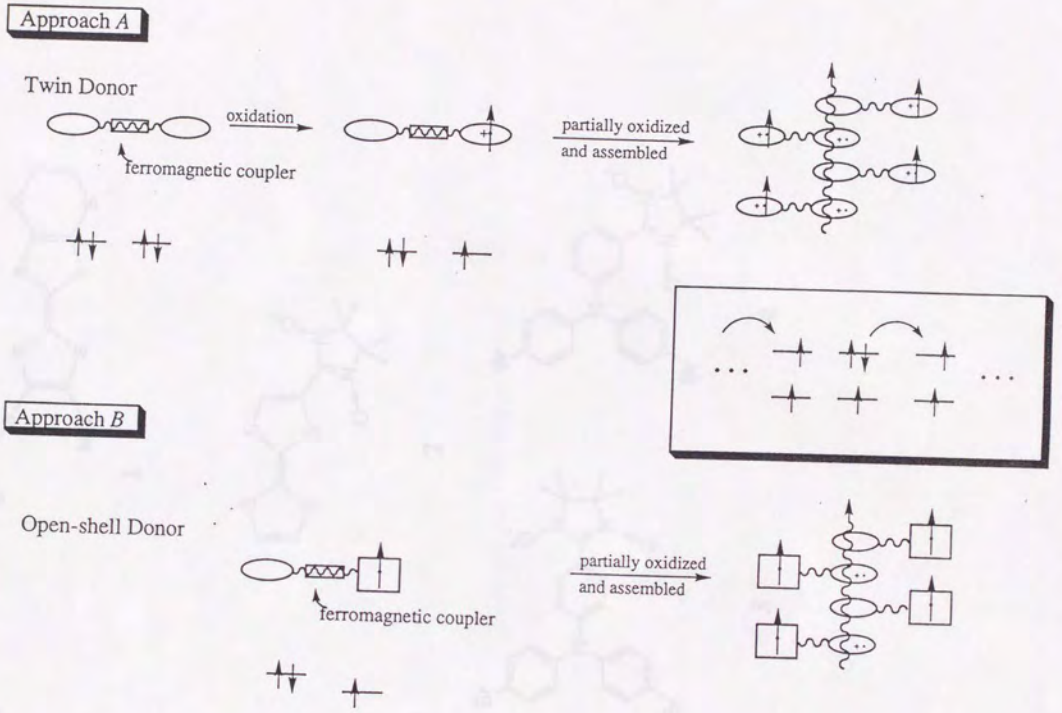

Figure I-4 Two approaches to construct organic ferromagnetic metals

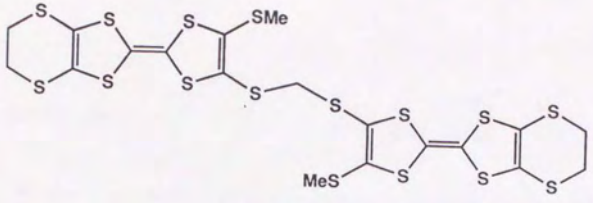

1

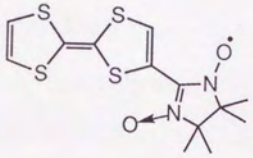

2

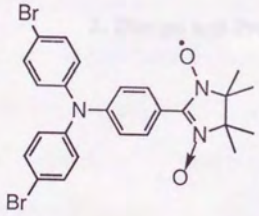

3

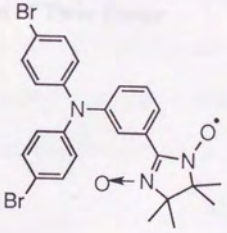

4

2. Design and Preparation of Twin Donor

2-1. Introduction

Physical properties of organic molecular crystals depend heavily on crystal structures and electronic features of constituent molecules. If a suitable arrangement in crystal is achieved, one can realize organic conductors with ferromagnetic property. Wudl proposed a concept of an organic ferromagnetic metal consist of partially oxidized donors with degenerated HOMO's (Figure II-1)[8]. This type of organic ferromagnetic metal may be classified as an organic counterpart of 3*d* metals in which localized spin and itinerant electrons are not distinguished. On the other hand, Breslow proposed an organic ferromagnet derived from CT interaction between a donor with degenerated HOMOs and an acceptor of an appropriate reduction potential[9]. Breslow utilized π-conjugated donors with high symmetry, such as triphenylenes, or hexaaminobenzene derivatives etc. Since such a π-system suffer from Jahn-Teller distortion heavily in the crystalline environment, the desired electronic structure has not been achieved due to a removal of degeneracy of HOMOs. Considering such a circumstance, the author designed a twin donor where two BEDT-TTF (ET) units are linked by a methylenedithio group[10]. Structural and electronic features of twin donors are as follows.

First, the unpaired electron is mainly localized in one of the donor

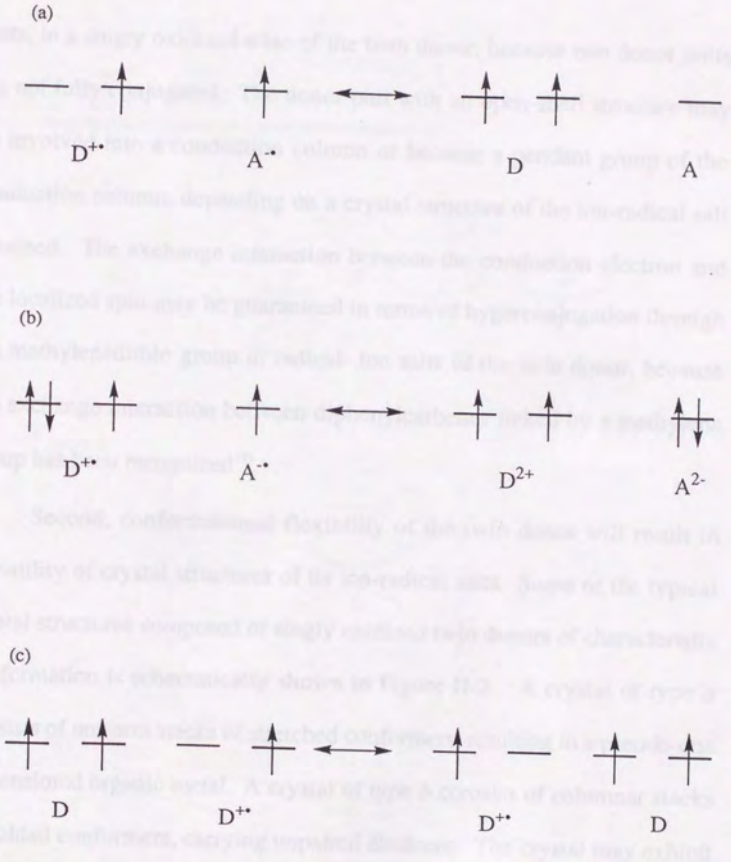

Figure II-1 Models of organic ferromagnetic metal
(a) McConnell model (b) Bleslow's modification
(c) Wudl's modification.

units, in a singly oxidized state of the twin donor, because two donor units are not fully conjugated. The donor part with an open-shell structure may be involved into a conduction column or become a pendant group of the conduction column, depending on a crystal structure of the ion-radical salt obtained. The exchange interaction between the conduction electron and the localized spin may be guaranteed in terms of hyperconjugation through the methylenedithio group in radical- ion salts of the twin donor, because the exchange interaction between diphenylcarbenes linked by a methylene group has been recognized[11].

Second, conformational flexibility of the twin donor will result in versatility of crystal structures of its ion-radical salts. Some of the typical crystal structures composed of singly oxidized twin donors of characteristic conformation is schematically shown in Figure II-2. A crystal of type *a* consists of uniform stacks of stretched conformers, resulting in a pseudo-one dimensional organic metal. A crystal of type *b* consists of columnar stacks of folded conformers, carrying unpaired electrons. The crystal may exhibit a magnetic property. While a crystal of type *c* consists of columnar stacks of stretched conformers, having pendant groups with a localized spin. This is the crystal structure which may exhibit a conduction property together with ferromagnetism.

Third, the presence of two donor units provides the twin donor with

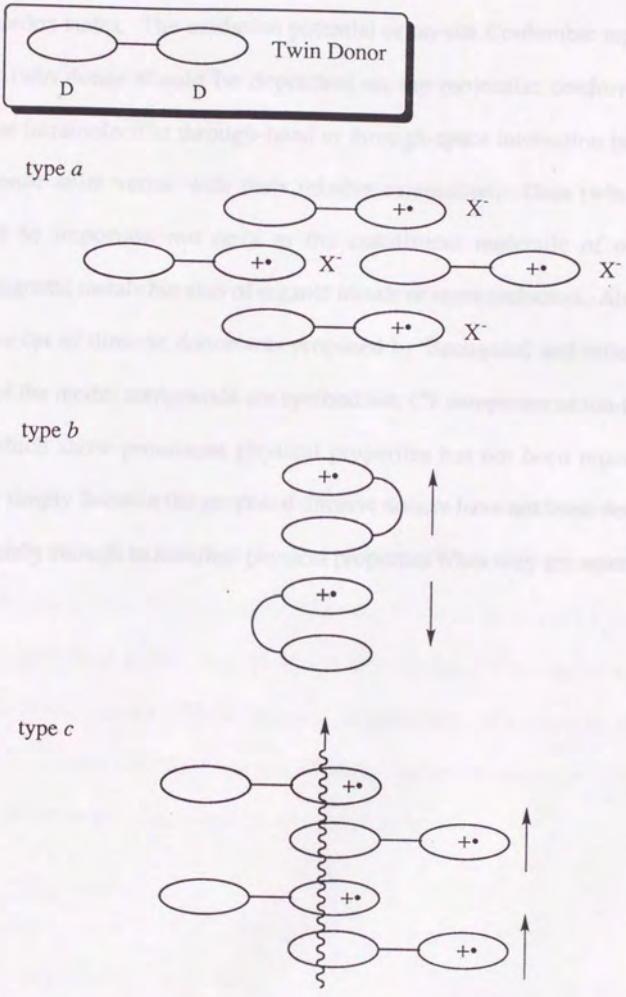

Figure II-2 Schematic drawing of crystal structure of twin donor ion radical salt.

multi-redox states. The oxidation potential or on-site Coulombic repulsion of the twin donor should be dependent on the molecular conformation, because intramolecular through-bond or through-space interaction between two donor units varies with their relative orientation. Thus twin donor should be important not only as the constituent molecule of organic ferromagnetic metals but also of organic metals or semiconductors. Although the concept of dimeric donor was proposed by Bechgaard and others and some of the model compounds are synthesized, CT complexes or ion-radical salts which show prominent physical properties has not been reported[12]. This is simply because the proposed dimeric donors have not been designed sufficiently enough to manifest physical properties when they are assembled.

2-2. Preparation of Twin Donor and Its Electrochemical Property

The twin donor **1** was prepared as shown in Scheme II-1. A hybrid sulfide (**6**) is the key compound to prepare unsymmetrically substituted TTF derivatives. The twin donor **1** was obtained by an usual cross-coupling method from diketone **8**. Separation of **1** was performed by gel-permeation chromatography and the isolated product was recrystallized from benzene:methanol (3:1 v/v).

Cyclic voltammogram of **1** showed reversible potential waves of the first and second redox processes; $E^1_{1/2} = 0.47$ V and $E^2_{1/2} = 0.55$ V, respectively. The splitting of the waves indicates that two TTF moieties interact in terms of a through-bond and/or through-space mechanism. The results suggest that the donor ability of twin donor **1** is practically the same as that of BEDT-TTF ($E_{1/2} = 0.52$ V measured under the same condition), except for the presence of intramolecular electronic interaction.

Scheme II-1

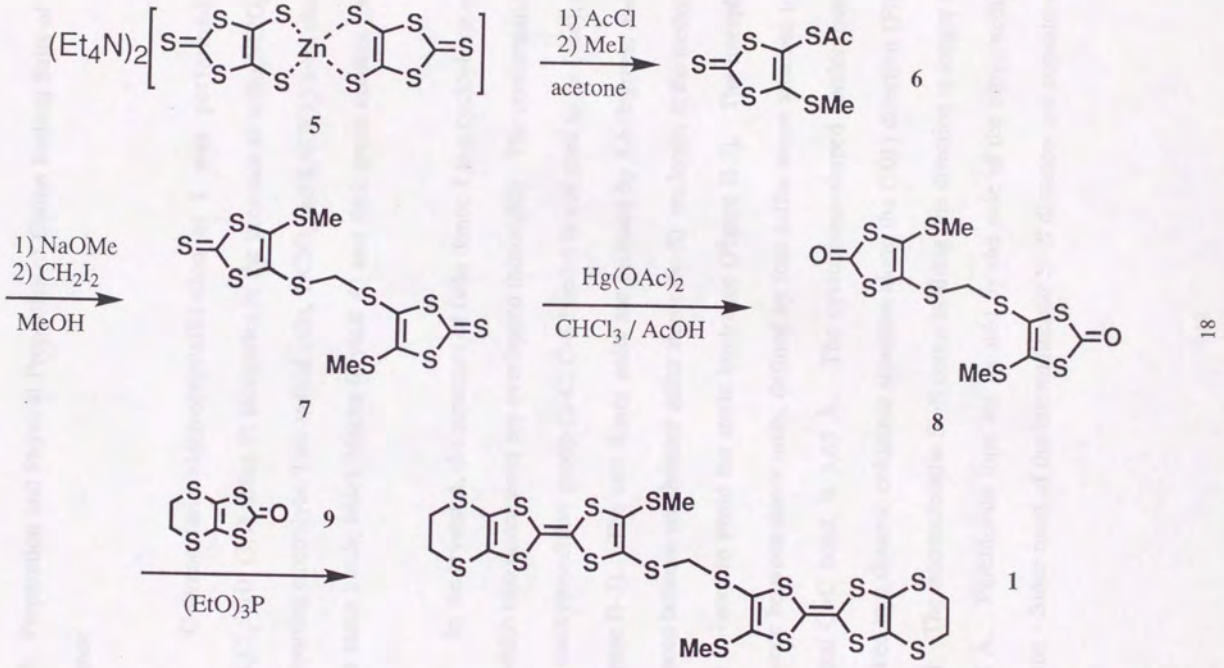
(Et4N)2
Zn
1) AcCl
2) MeI
acetone
SAc
SMe
6
5
1) NaOMe
2) CH2I2
MeOH
7
Hg(OAc)2
CHCl3 / AcOH
8
9
(EtO)3P
1

2-3. Preparation and Physical Properties of Cation Radical Salts of Twin Donor

Galvanostatic electrocrystallization of **1** was performed in CH_2Cl_2:THF (3:1) using Pt electrodes in the presence of n-Bu_4NClO_4 as a supporting electrolyte. Two radical salts, **1**•ClO_4 and $\mathbf{1}_2$•(ClO_4) were obtained in a same batch; black blocks (crystal *A*) and dark green needles (crystal *B*).

In the crystal *A*, the structure of twin donor **1** is a cyclophane-shape in which two donor units are overlapped thoroughly: The conformation of the methylenedithio group (S-C, C-S bonds) is assigned to be (+sc), (-sc) (Figure II-3). The two donor units are inclined by 8.6 degrees, and the distance between non-bonded sulfur atoms (S···S) are longer at the methylthio side in order to avoid the steric hindrance (Figure II-3). The interplanar distance between donor units, defined by four sulfur atoms attached to the central C=C bond, is 3.65 Å. The cyclophane-shaped conformers are stacked in a dimeric columnar structure along the (101) direction (Figure II-4). The intermolecular S···S contacts along this direction is longer than 3.65 Å. Perchlorate ions are located by the side of the ethylenedithio groups. Since most of the intermolecular S···S distances are considerably

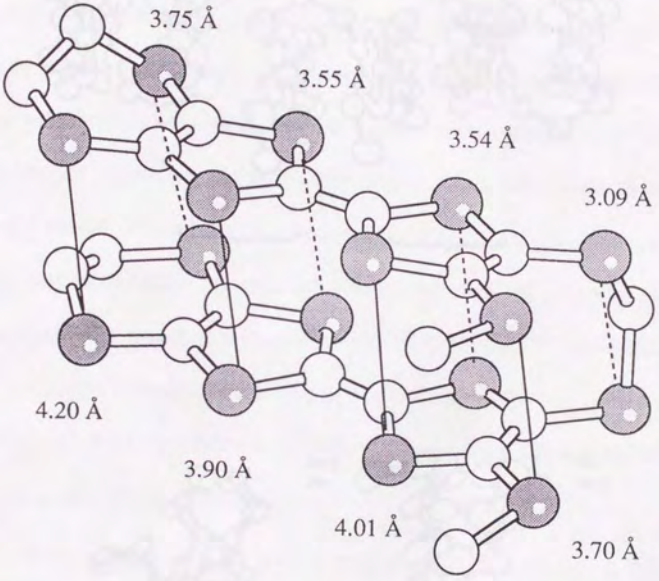

Figure II-3 Molecular structure of $\mathbf{1}^{+\bullet}$ in $\mathbf{1}\bullet ClO_4$ (Crystal *A*)

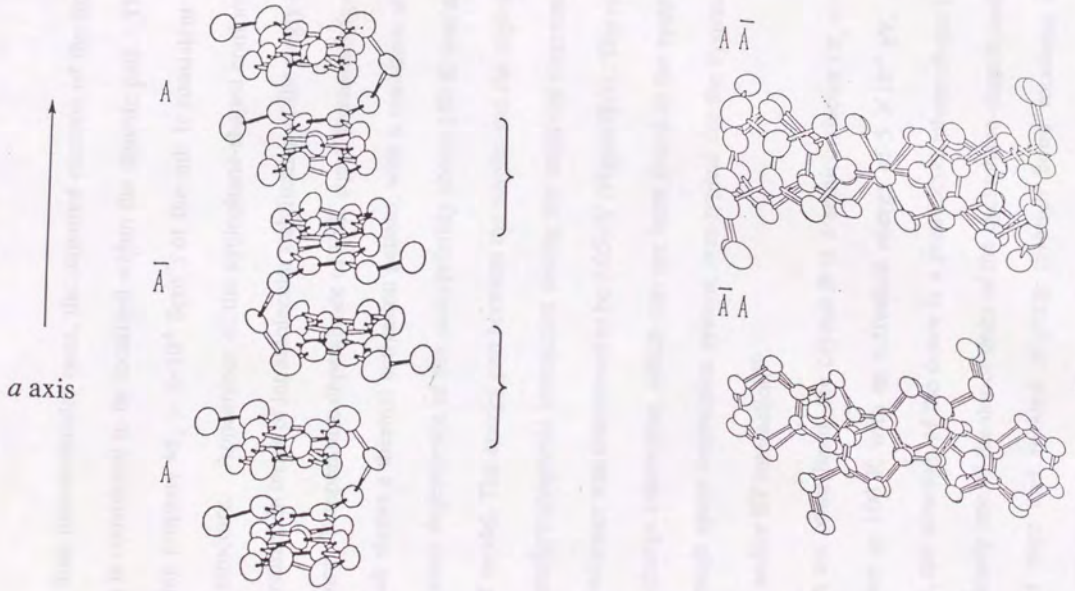

Figure II-4 Column structure of **1**·ClO_4.

longer than intramolecular ones, the unpaired electron of the ion radical species is considered to be localized within the dimeric pair. The nearly insulating property (σ_{rt} = 1×10^{-8} Scm^{-1}) of the salt is consistent with the crystal structure. Appearance of the cyclophane-shaped conformer may be rationalized in terms of intramolecular stabilization of the singly-oxidized twin donor. Temperature dependence of ESR signal intensities (g=2.0062) of the salt shows a thermal activation pattern, with a transition at 150 K. Temperature dependence of the susceptibility above 150 K was analyzed by a S-T model. The energy gap between the singlet and the triplet caused by the antiferromagnetic interaction among the unpaired electrons of the phane conformer was determined to be 0.05 eV (Figure II-5). The relatively large exchange interaction, which can not been found in the system only with through space interaction system, was typical for the system which have CT and/or ET interaction[13].

On the other hand, the crystal *B* is a semiconductor (σ_{rt} = 0.15 S cm^{-1}) down to 100 K with an activation energy of 5 $\times10^{-2}$ eV. In the crystal *B*, the structure of the donor is a pseudocyclophane-shape (Figure II-6). Namely one of the donor units of the cyclophane-shaped conformer is turned over and rotated slightly through bond rotations of the methylenedithio chain: the conformation of the methylenedithio group (S-C, C-S bonds) is (+sc), (+sc). The pseudocyclophane-shaped conformers are

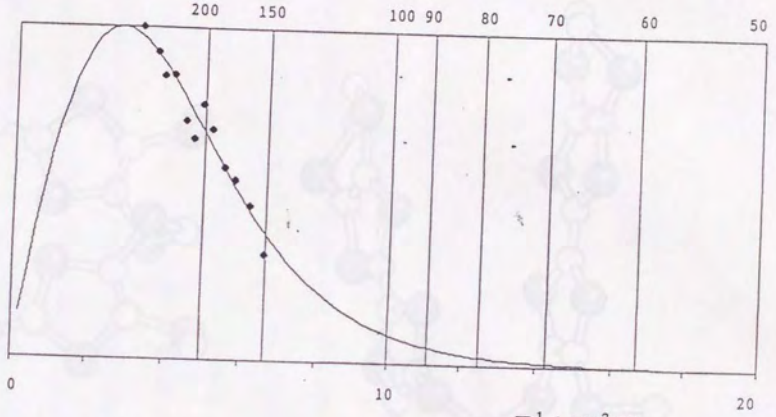

Figure II-5 Temperature dependence of ESR signal intensity of **1**·ClO_4.

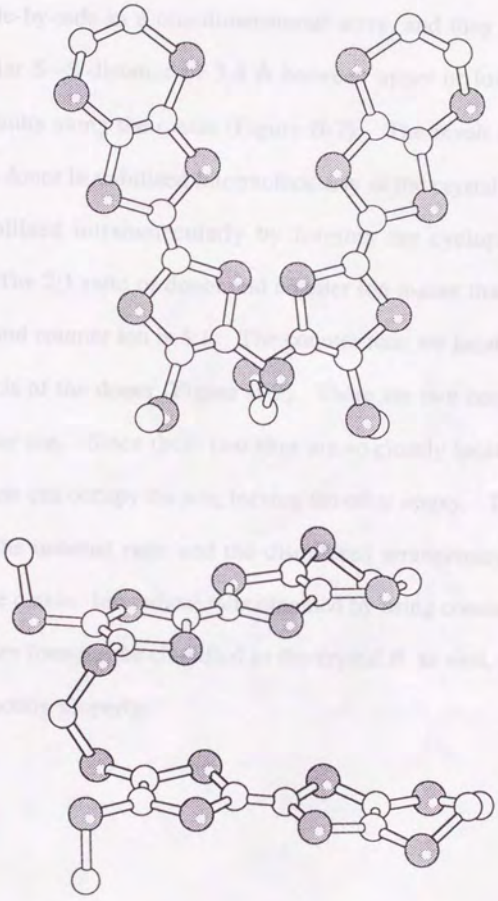

Figure II-6 Molecular structure of $\mathbf{1}^{\frac{1}{2}+\bullet}$ in $\mathbf{1}_2 \bullet ClO_4$ (Crystal *B*)

arranged side-by-side in a one-dimensional array, and they have a short intermolecular S···S distance of 3.4 Å between upper or lower edges of each donor units along the *c* axis (Figure II-7). The result suggests that the oxidized donor is stabilized intermolecularly in the crystal *B* salt rather than be stabilized intramolecularly by forming the cyclophane-shaped conformer. The 2:1 ratio of donor and counter ion means that the ratio of donor units and counter ion is 4:1. The counter ions are located on the C_2 symmetry axis of the donor (Figure II-7). There are two occupying sites for the counter ion. Since these two sites are so closely located that only one counter ion can occupy the site, leaving the other empty. This situation rationalizes the unusual ratio and the disordered arrangement of counter ions along the *c* axis. Ion radical salts obtained by using counter ions, such as BF_4^-, I_3^-, are found to be classified as the crystal *B* as well, exhibiting a similar conducting property.

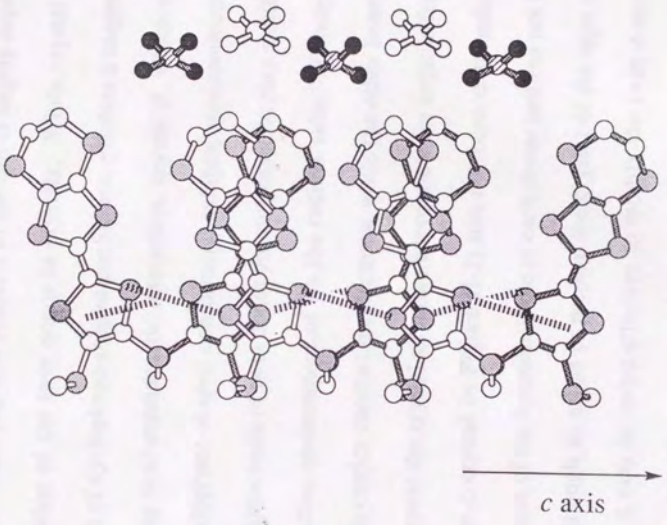

Figure II-7 Crystal structure of $\mathbf{1}_2 \cdot ClO_4$. S···S contacts of 3.4Å are shown by dotted lines. Occupancy of counter anion is 0.5.

2-4. Summary

By utilizing the novel twin donor, the author succeeded to prepare ion-radical salts which exhibit intriguing physical properties. Especially it is to be noted that physical property of the salt is largely dependent on the conformation of the twin donor in crystals. While crystal *A*, which is composed of cyclophane-shaped conformer, exhibits a magnetic property with strong antiferromagnetic interaction, crystal *B*, which composed of pseudocyclophane-shaped conformers, exhibits semiconducting property. The two donor units of twin donor are supporsed to play a different role in the crystalline environment of its ion radical salts. Namely one of the donor units carries conduction electrons, while the other bears a localized spin. However the crystal structure appropriate for organic ferromagnetic metal (type *c* crystal in Figure II-2) has not been obtained. Therefore discrimination of the functional role of each donor unit can not be achieved so far. Although an effort to prepare the crystal of the type *c* should be continued, it may be more effective to modify the twin donor. Namely replace one of the donor units with a stable radical unit.

2-5. Experimental

1) General Procedures.

^{1}H NMR spectra were measured by JEOL GSX-270 (270 MHz) and JEOL α-500 (500 MHz) spectrometer, on which chemical shifts in $CDCl_3$ solutions were reported in δ relative to Me_4Si as an internal standard. Infrared spectra were recorded by a Perkin Elmer 1400 series infrared spectrometer using a KBr pellet. Gel permeation chromatgraphy was performed by LC-908 (Japan Analytical Industry co., ltd.) equipped with JAIGEL-1H and 2H columns. Chloroform was used as an eluent. Cyclic voltammograms (CV) were measured in dichloromethane in the presence of tetra-n-butylammonium perchlorate as an electrolyte with a platinum working electrode using a potentiostat/galvanostat HAB 151 (HOKUTO DENKO Ltd.). An Ag/AgCl electrode was used for a reference electrode. Scanning rate was 200 mVs^{-1}. ESR measurements were carried out with an X-band ESR spectrometer (JEOL JES-RE2X), with a modulation of 100 kHz. Resonance fields were measured by an NMR field meter (JEOL ES-FC5). Frequency of microwave was recorded by an ADVANTEST TR5212 meter.

2) Materials

Zinc chelate[14] (**5**) and 1,3,-dithiol-2-ketone derivatives[15] (**9**) were prepared according to the published procedures. THF was distilled over sodium metal and benzophenone immediately prior to use. Methanol was distilled from sodium. Triethylphosphite was treated with sodium, then decanted and distilled. All distillation procedures were performed under a nitrogen atmosphere. Acetone was dried over K_2CO_3. All other reagents were used as purchased without further purification.

3) Preparation

4-Acetyltio-5-methylthio-1,3-dithiol-2-thione (**6**): To a solution of Zinc chelate (7.24 g, 10.0 mmol) of acetone, a mixture of acetylchloride (1.58 g, 20.1 mmol) and acetone (25 ml) was added under a nitrogen atmosphere at 0 °C, then the mixture was stirred for 2.5 hours at room temperature. To the reaction mixture, 4.3g (30.3 mmol) of methyliodide was added and the mixture was stirred for 3 hours. The reaction mixture was cooled and filtrated, then filtrate was evaporated under a reduced pressure. The residue was treated with carbontetrachloride, then filtrated, and the filtrate was evaporated under a reduced pressure. Recrytallization of the residue from benzene-hexane gave red powder; Yield 45 % (2.31 g, 9.08 mmol); ^{1}H-NMR

($CDCl_3$) δ = 2.46 (s, SCH_3, 3H), 2.50 (s, $COCH_3$, 3H).

Bis(2-thioxo-5-methylthio-1,3,-dithiol-4-thio)methane (7): In a 100 ml round-bottomed flask, 2.00 g (7.86 mmol) of **6** and 80 ml of dry methanol were added. To this suspension, solution of sodium methoxide (1.52 g of 28 % methanol solution) was added dropwise with stirring at room temperature under a nitrogen atmosphere. The reaction mixture was stirred for 30 minutes, then diiodomethane (1.00 g 3.73 mmol) was added dropwise with stirring and the mixture was further stirred overnight. Brownish yellow powders precipitated, which were collected by filtration and washed with water and methanol, and dried. Crystallization from chloroform solution gave pure yellow powder; Yield 64 % (1.10 g, 2.52 mmol), ^{1}H-NMR ($CDCl_3$) δ = 4.2 (s, $-CH_2-$, 2H), 2.5 (s, $-SCH_3$, 3H); IR (KBr) 1030 cm^{-1} (C=S), 1209, 1363, 1422, 1458 (C=C), 2960 (CH).

Bis(2-oxo-5-methylthio-1,3,-dithiol-4-thio)methane (8): Dithione 7 (3.42 g, 7.83 mmol) and $Hg(OAc)_2$ (25.48 g, 86.47 mmol) was dissolved in a mixture of chloroform (200 ml) and acetic acid (100 ml) and the solution was stirred for 3 hours at room temperature. The reaction mixture turned to a white emulsion. Then the reaction mixture was filtrated, and the filtrate was transferred to a separate funnel and extracted with chloroform

several times. Combined organic layers were washed with water (200ml x 5) and $NaHCO_3$ aq (200ml x 3), and water (200ml x 2), successively. The organic layer was separated and dried over $MgSO_4$, and the solvent was removed by evaporation and the residue was recrystallization from benzene-hexane; Yield 47 % (1.48 g, 3.66 mmol), ^{1}H-NMR ($CDCl_3$) δ = 4.2 (s, -CH_2-, 2H), 2.5 (s, -SCH_3, 3H); IR (KBr) 1203 cm^{-1}, 1430, 1470 (C=C), 1617, 1664 (C=O), 2921 (CH).

Bis(4',5'-ethylenedithio-5-methylthio-tetrathiafulvalenyl-4-thio)methane (1): Under a nitrogen atmosphere diketone **8** (1.48 g, 3.66 mmol) and 4,5-ethylenedithio-1,3-dithiol-2-one (4.57 g, 21.93 mmol) in triethylphosphite (40 ml) were reacted under reflux for 30 minutes. The reaction mixture was cooled and diluted with methanol. The orange powder was filtrated and washed with methanol and dried under a reduced pressure. The resulting reaction mixture was separated by gel-permeation chromatography. Obtained twin donor **1** was purified by recrystallization from a benzene-methanol (3:1 v/v); Yield 17 % (471 mg, 0.622 mmol); mp 170~173 °C (dec.); ^{1}H-NMR ($CDCl_3$) δ = 2.6 (s, -SCH_3-, 6H), 3.3 (s, -SCH_2CH_2S-, 8H), 4.25 (s, -SCH_2S-, 2H); IR (KBr) 1286 cm^{-1}, 1419(C=C), 2914 (CH); Anal found Calc. for $C_{19}S_{16}H_{16}$: C 30.14 %, H 2.13, S 67.74, Obs. : C 30.42 %, H 2.18, S 67.46.

4) Electrocrystallization

Twin donor **1** (10.0 mg, 0.013 mmol) and tetra-n-butylammonium perchlorate (171 mg, 0.5 mmol) were placed in the anodic side and tetra-n-butylammonium perchlorate (171 mg, 0.5 mmol) in the cathodic side of a 20 ml H-type cell. Under a nitrogen atmosphere dichloromethane (5 ml) and THF (15 ml) was added to each side of the cell and stirred magnetically for 1 hour. Galvanostatic electrocrystallization was achieved at electric current of 0.5 μA.

5) Electrical conductivity measurement

The electric conductivity was measured by a four probe method. Along the long axis of the sample gold wire (25 μm ϕ) were attached to the sample with gold paint as a contact. The sample was fixed in a chamber in homemade cryostat and was cooled slowly. The temperature was measured by using an Fe-Au-Chromel thermocouple.

6) X-ray crystal structure analysis

$1 \cdot ClO_4$ (Crystal *A*)

The sample for the X-ray analysis was obtained by galvanostatic electrocrystallization (0.5 μA) using 20 ml H-type cell and Pt electrode; a black block crystal with dimensions $0.20 \times 0.15 \times 0.05$ mm. The intensity data collection was measured at ambient temperature on a Rigaku AFC-5 four-circle diffractometer by using graphite-monochromatized MoKα radiation; scan speed $4°min^{-1}$. Three standard reflections ($\bar{3}\,2\,\bar{1}$, $\bar{2}\,4\,1$, $\bar{2}\,1\,5$) were measured for every 100 reflections and showed no significant variations throughout the data collection; 7184 reflections ($4° \leq 2\theta \leq 50°$) measured, 2896 independent reflections ($Fo \geq 3\sigma(Fo)$) were used for analysis ($R_{int} = 0.053$).

Structure solved by direct methods using *SAPI-85* (Fan, Qian, Yao, Zheng & Hao, 1988), a block diagonal least-squares refinement (on F), scattering factors from *International Tables for X-ray Crystallography* (1974). Calculations carried out on a FACOM A-70 with *UNICS III* (Sakurai & Kobayashi, 1979). Final refinement with anisotropic thermal factors for all non-hydrogen atoms; 361 parameters, R = 0.082.

$1_2 \cdot ClO_4$ (Crystal *B*)

The sample for the X-ray analysis was obtained by galvanostatic electrocrystallization (0.5 μA) using 20 ml H-type cell and Pt electrode; a greenish black block crystal with dimensions $0.60 \times 0.20 \times 0.08$ mm. The intensity data collection was measured at ambient temperature on a Rigaku AFC-5 four-circle diffractometer by using graphite-monochromatized MoKα radiation; scan speed $4°min^{-1}$. Three standard reflections (4 0 0, 2 12 1, 1 7 3) were measured for every 100 reflections and showed no significant variations throughout the data collection; 3484 reflections ($4° \leq 2\theta \leq 50°$) measured, 1958 independent reflections ($Fo \geq 3\sigma(Fo)$) were used for analysis ($R_{int} = 0.053$).

Structure solved by direct methods using *SAPI-85*, a block diagonal least-squares refinement (on F), scattering factors from *International Tables for X-ray Crystallography* . Calculations carried out on a FACOM A-70 with *UNICS III*. Final refinement with anisotropic thermal factors for all non-hydrogen atoms; 262 parameters, R = 0.083.

3. Design and Preparation of Open-Shell Donors

3-1. Design of Open-Shell Donors

In order to construct organic ferromagnetic metal, the twin donor should be modified to have two functionalities separately. Namely the author designed an open-shell donor in which a stable radical is introduced to the donor part through a cross-conjugated system. It is to be noted that the cross-conjugation is inevitable for maintaining two types of unpaired spins regardless the spin state of cation biradical which is formed by one-electron oxidation. The stable radical moiety is supposed to bear a localized spin and the donor moiety is to carry conduction electrons when the open-shell donor is partially oxidized. Although some open-shell donors have been reported[16], information on the intramolecular exchange interaction in the singly oxidized state has not been discussed at all.

A cation biradical of the open-shell donor has two types of spin source derived from two non-degenerate SOMOs. The cation biradical can be considered as a novel ground state triplet species, if two spins are ferromagnetically coupled. Development of organic ground state triplet species is of greatly important not only from the view point of construction of organic magnetic materials but also from spin chemistry in general. All of the ground state triplet species reported hitherto can be classified into two categories: one is one-centered biradicals, such as carbenes[17] or

nitrenes[18], having two nearly degenerated SOMOs at one-center, and another is cross-conjugated biradicals, such as trimethylenemethane[19] (TMM), *m*-xylylene[20], and their charged radical analogue[21], having two degenerated SOMOs at two centers. The cation radical of open-shell donor cannot be classified into either of them and should be considered as a different spin system in this respect.

In general, biradical which consists of a radical cation of donor and localized spin becomes non-degenerate system. Following conditions are required for such a non-degenerate two centered biradical to become a ground state triplet. First, the energy level of HOMO should be higher than that of SOMO so that the oxidation occurs from the donor moiety as shown in Figure III-1. Therefore it is necessary to choose the donor moiety with relatively high donor ability. Second, one-oxidized singlet state of the open-shell donor has three electronic configurations, S_1, S_2, and S_3 whereas the triplet has only one configuration which is the biradical structure shown by T_0. When the relative stability of each state is considered, taking the S_1 state as a standard, the T_0 state should exist below S_1 based on the exchange interaction (Kss'). On the other hand, S_2 is stabilized by the orbital energy $\Delta\varepsilon$, compared with S_1, but is destabilized by Coulombic repulsion (U_s) because two electrons exist in the same orbital. Then, according to the balance between the two, the S_2 state can be located either above or below the S_1 state. While the S_3 state is always more unstable than S_1 and

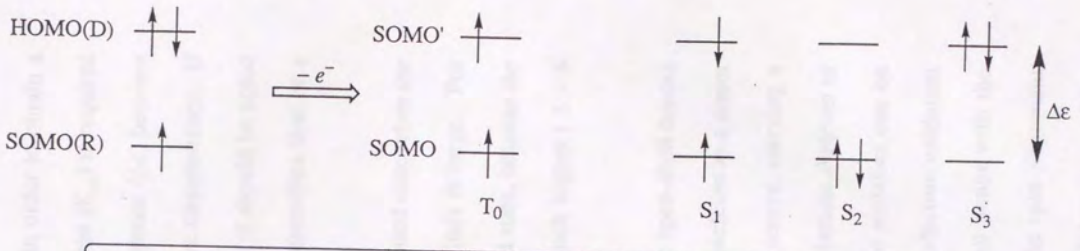

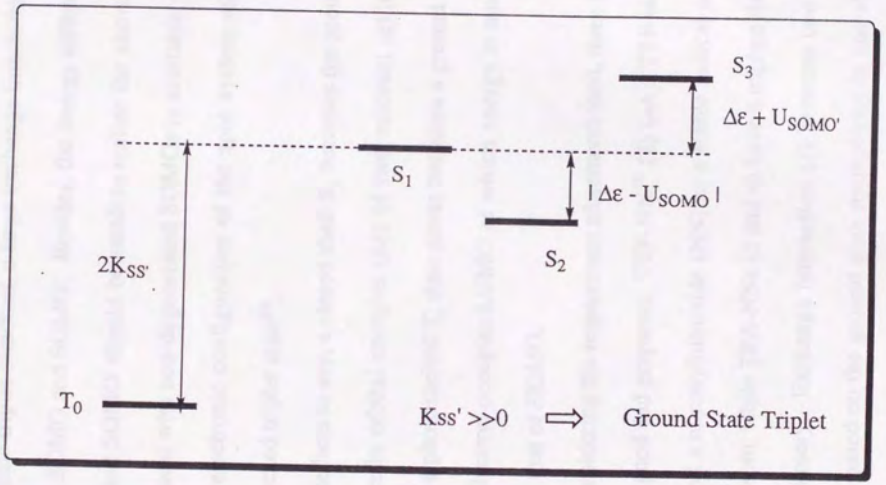

Figure III-1. Electronic structure and energy diagram of one-oxidation state of open-shell donor

S_2, because both the orbital energy and Coulombic repulsion is unfavorable for stabilizing the energy of the S_1 state. Therefore, in order to obtain a ground state triplet biradical, a large exchange interaction ($K_{ss'}$) is required between SOMO and SOMO'. Besides, the energy difference ($\Delta\varepsilon$) between SOMO and SOMO' should be small to realize the above circumstance. If the biradical with non-degenerated SOMOs is available, it should be noted that the electronic configuration of the spin system resembles that of a photo-excited triplet state[22].

Needless to say, a closed shell S_1 becomes the ground state when the difference in orbital energies ($\Delta\varepsilon$) of two relevant orbitals is large. For instance, a photoexcited T_1 state never becomes a ground state, because the excited electron occupies LUMO of which energy is much higher (3 ~ 4 eV) than that of HOMO.

Considering the requirement aforementioned, three open-shell donors were designed and prepared. TTF-NN[23] (**2**) has a TTF skeleton as a donor moiety and a nitronylnitroxide (NN) as a stable radical source, carrying a localized spin, while TPA-NNs (**3** and **4**) have a triphenylamine skeleton as a donor moiety. Exchange interaction (*J*) between two moieties can be estimated based on the ground state multiplicity in one-electron oxidation state of these open-shell donors. In the case open-shell donor with the triphenylamine skeleton **3** and **4**, it is expected that the spin alignment mechanism may be obtained by comparing the exchange interactions of the

para and *meta* substituent.

3-2. Preparation of TTF-NN

An open-shell donor which have a TTF moiety, TTF-NN (**2**) was synthesized as shown in Scheme III-1. Formyl-TTF[24] (**10**) was reacted with 2,3-dimethyl-2,3-bishydroxylaminobutane[25] (**11**), and the resulted adduct was oxidized by PbO_2 to give **2** (m.p 77.9 °C (dec.)). Generally speaking, a substituted NN is prepared from a formyl derivative, but formyl-TTF is not reactive because of contribution of intramolecular charge-transfer. Then formyl-TTF can not be reacted with bishydroxylamine in a normal condition. After checking various solutions, non-polar solvents are found to be effective to promote the reaction. The cyclic hydroxylamine (**12**) was oxidized by PbO_2 in THF to give an open-shell donor TTF-NN, **2**. The open-shell donor **2** was purified by silicagel column chromatography at low temperature (-30°C). Once purified, **2** is relatively stable, but decomposes slowly in the air at room temperature.

The instability of the neutral open-shell donor makes the preparation of the CT complex difficult. The stability of the donor may be increased by introducing a methylthio (or methyl) group as the protection of the double bond, because the instability may come from the close location between the double bond and nitroxide radical.

The IR and mass spectral data of **2** are consistent with the desired

Scheme III-1

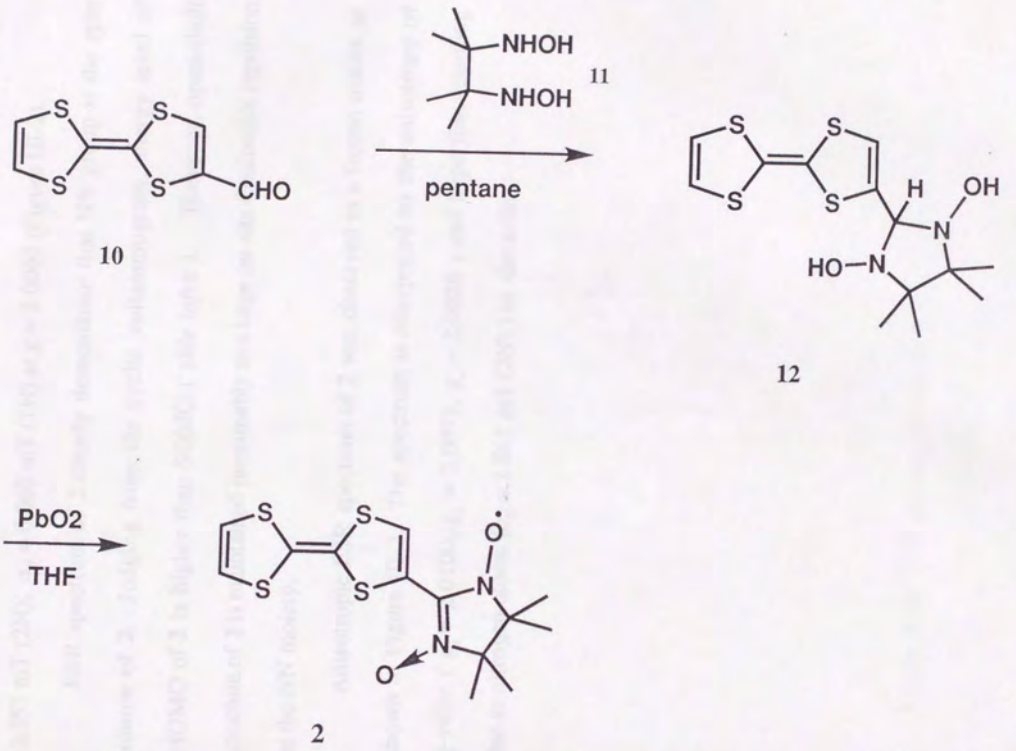

structure. ESR spectrum of **2** in benzene shows double quintets with a_N = 0.757 mT (2N), a_H = 0.060 mT (1H) at g = 2.0063 (Figure III-2).

ESR spectrum of **2** clearly demonstrate that NN group is the spin source of **2**. Judging from the cyclic voltammogram, energy level of HOMO of **2** is higher than SOMO (*vide infra*). However, open-shell structure of **2** is maintained presumably to a large on-site Coulombic repulsion at the NN moiety.

Anisotropic ESR spectrum of **2** was observed in a frozen matrix as shown in Figure III-3. The spectrum is interpreted by the anisotropy of g-value (g_x = 2.0100, g_y = 2.0073, g_z = 2.0026) and hyperfine coupling due to nitrogen atoms (a_N = 1.861 mT (2N)) in the z-line.

Figure III-2. ESR spectum of neutral **1** in benzene solution.

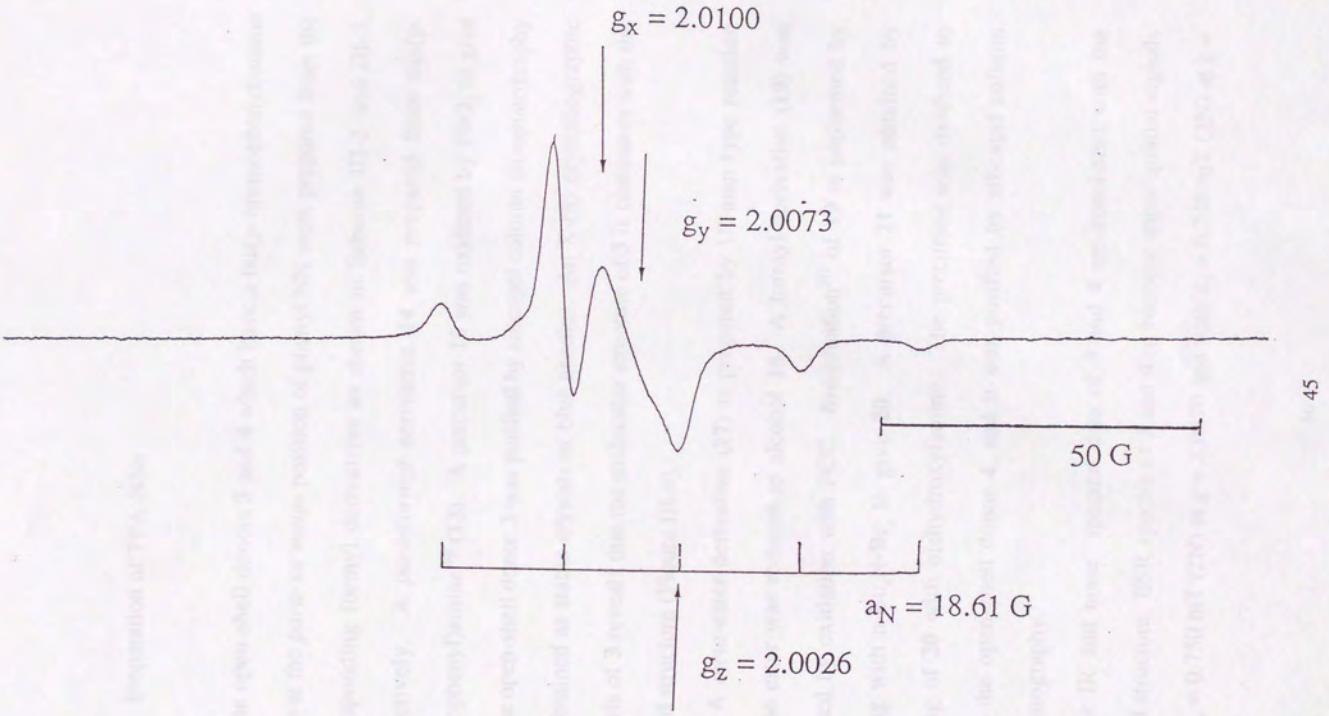

Figure III-3. ESR spectrum of 1 in MTHF glass

3-3. Preparation of TPA-NNs

The open-shell donors **3** and **4** which have a bis(*p*-bromophenyl)amino group at the *para*- or *meta*- position of phenyl NN were prepared from the corresponding formyl derivatives as shown in Scheme III-2 and III-3, respectively. A *para*-formyl derivative **14** was prepared from tris(p-bromophenyl)amine[26] (**13**). A precursor **15** was oxidized by PbO_2 to give **3**. The open-shell donor **3** was purified by silicagel column chromatography and obtained as stable crystals of blue needles. An X-ray crystallographic analysis of **3** reveals that the molecular structure of **3** is consistent with the desired structure (Figure III-4).

A *meta*-ester derivative (**17**) is prepared by Ullman-type reaction and the ester was reduced to alcohol **18**. A formyl-derivative (**19**) was obtained by oxidation with PCC. Bromination[27] of **19** is performed by treating with n-$Bu_4N{\bullet}Br_3$ to give **20**. A precursor **21** was obtained by treating of **20** with bishydroxylamine. The precursor was oxidized to afford the open-shell donor **4**, and it was purified by silicagel column chromatography.

The IR and mass spectral data of **3** and **4** are consistent with the desired structure. ESR spectra of **3** and **4** in benzene show quintet signals with a_N = 0.750 mT (2N) at g = 2.0070 and with a_N = 0.748 mT (2N) at g =

2.0070, respectively.

Scheme III-2

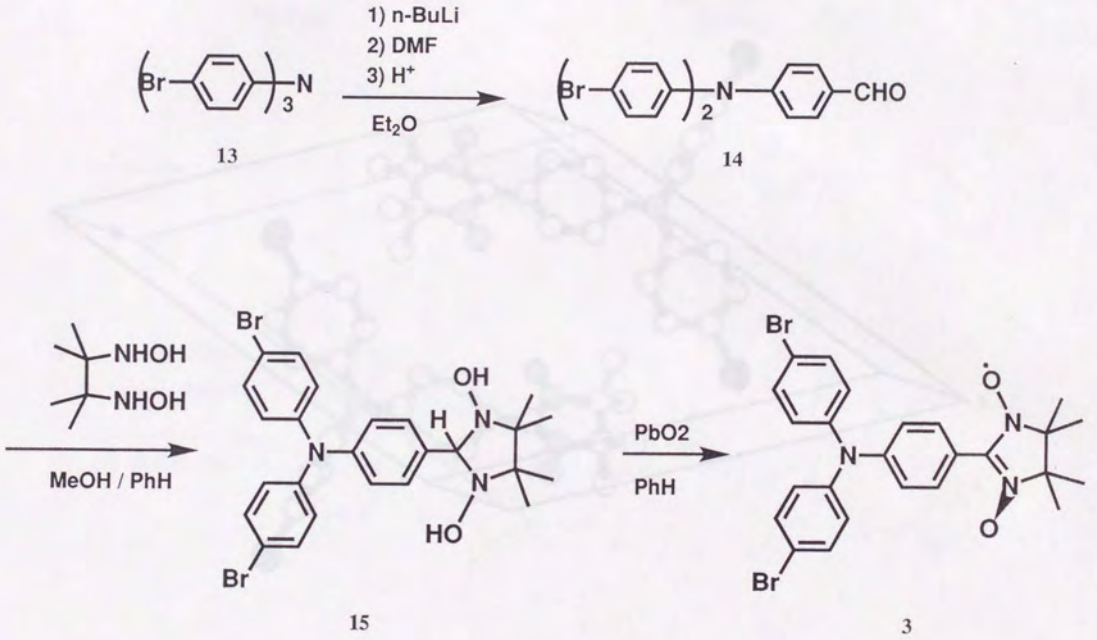

13 14

15 3

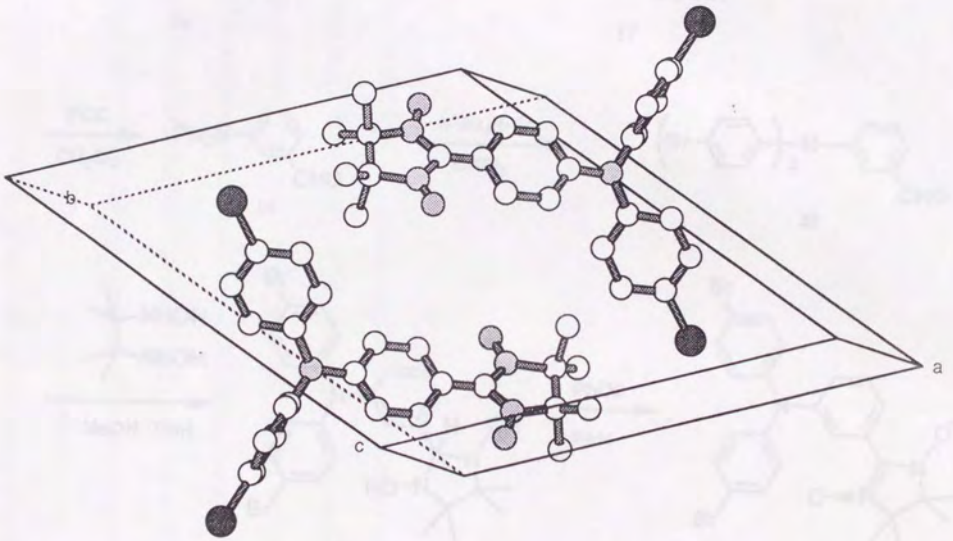

Figure III-4. Crystal structure of open-shell donor **2**.

Scheme III-3

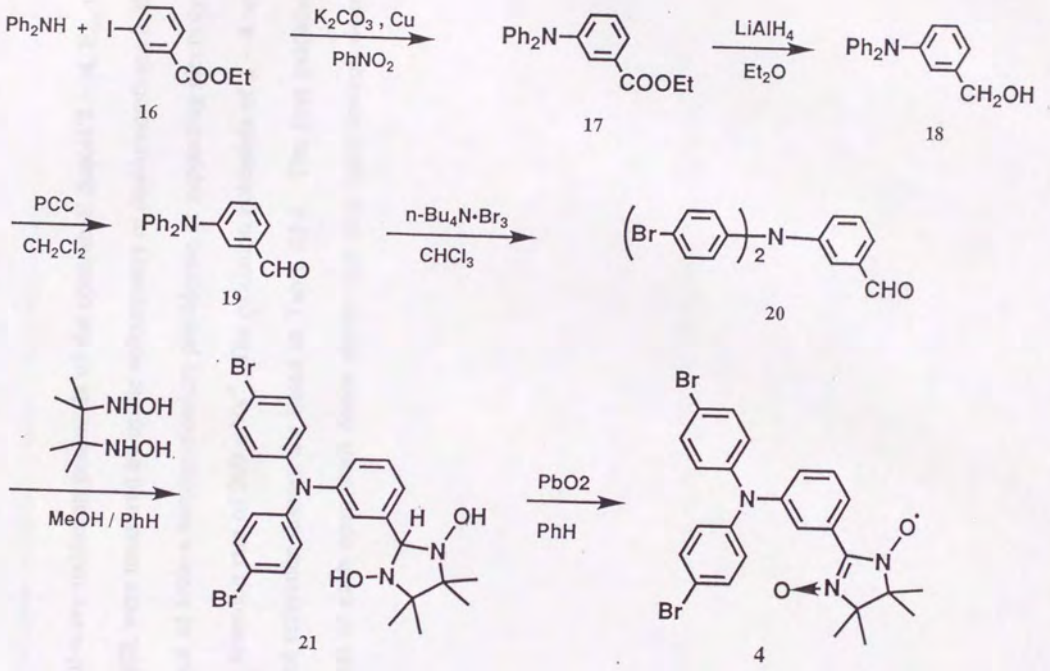
Ph2NH + I
COOEt
16
K2CO3 , Cu
PhNO2
Ph2N
COOEt
17
LiAlH4
Et2O
Ph2N
CH2OH
18
PCC
CH2Cl2
Ph2N
CHO
19
n-Bu4N·Br3
CHCl3
Br
2
N
CHO
20
NHOH
NHOH
MeOH / PhH
Br
N
H
OH
N
HO-N
Br
21
PbO2
PhH
Br
N
O
N
O
N
Br
4

3-4. Oxidation Potentials of Open-Shell Donors

Half-wave oxidation potentials of the open-shell donors **2** ~ **4**, $E_{1/2}$ *vs.* Ag/AgCl, were measured by cyclic voltammetry in dichloromethane in the presence of tetra-*n*-butylammonium perchlorate as supporting electrolyte with a scanning rate of 200 mVs^{-1}. The oxidation potentials of **2** ~ **4** and those of reference donors are listed in Table III-1. The first oxidation potential of each open-shell donor shows that they have enough donor ability.

	$E^{ox1}_{1/2}$	$E^{ox2}_{1/2}$	$E^{ox3}_{1/2}$
2	0.32	0.77(irrev.)	1.00(irrev.)
TTF	0.34	0.71(irrev.)	
3	0.82	1.38(irrev.)	
4	0.88	1.22(irrev.)	
$(p\text{-Br-}C_6H_4)_3N$	1.23		

(*V vs.* Ag/AgCl)

Table III-1. Oxidation potentials of open-shell donors.

3-5. Magnetic Properties of Neutral Open-Shell Donors (**2** ~ **4**)

Magnetic susceptibilities of the neutral open-shell donors were measured by a Faraday-type magnetic balance at temperatures between 3 K and 250 K. The χT *vs.* T plot is shown in Figure III-5, III-6 or III-7. Temperature dependence of the susceptibility of **2** shows a weak antiferromagnetic intermolecular interaction (θ = -1.2 K). The value of χT (= Curie constant) at 250 K (0.315 emuK/mol) shows that a part of neutral **2** decomposes and turned into a diamagnetic compound because of instability of the compound (*vide supra*).

Temperature dependence of the susceptibility of **3** or **4** also shows antiferromagnetic intermolecular interaction. Judging from the χT value at 250 K ($\approx$ 0.375 emuK/mol) spin concentration of **3** or **4** is almost 100 %.

The χT-T plot of **3** can be reproduced reasonably well by theoretical curve on a molecular field apploximation in terms of θ = -3 K. Crystal structure of **3** indicates the proximal location of O•••O atoms (with an intermolecular O•••O distance of 3.53 Å) (Figure III-8). This geometrical feature may result in an intermolecular antiferromagnetic interaction. Besides, intermolecular distance between phenyl group and oxygen atom is relatively short (3.29 Å). Since spin distribution of NN is mainly localized in O-N-C-N-O moiety, the magnetic interaction at this site would be

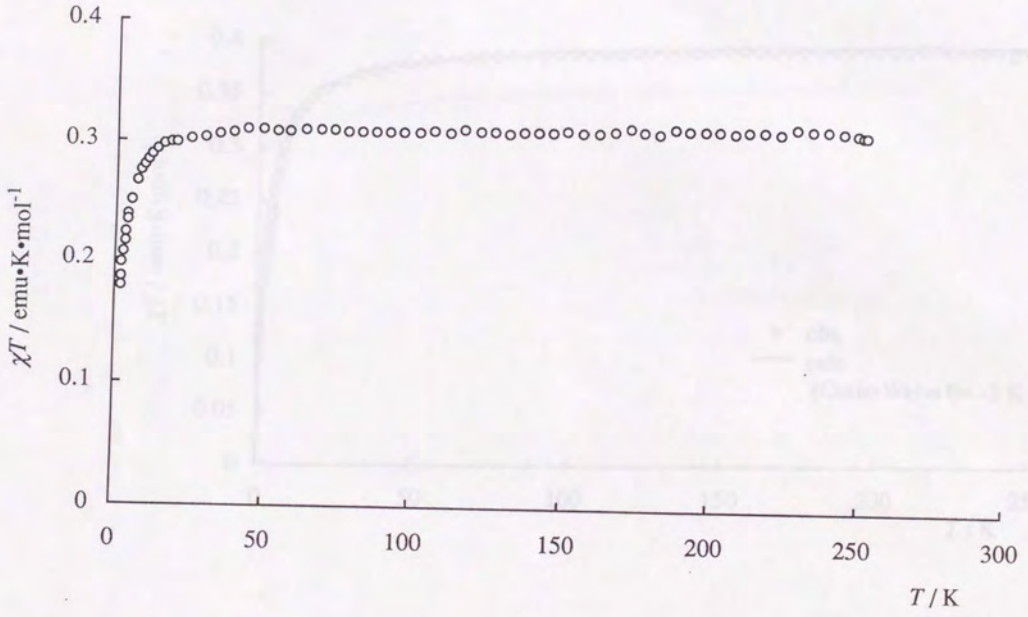

Figure III-5. χT-T plot of neutral **2**.

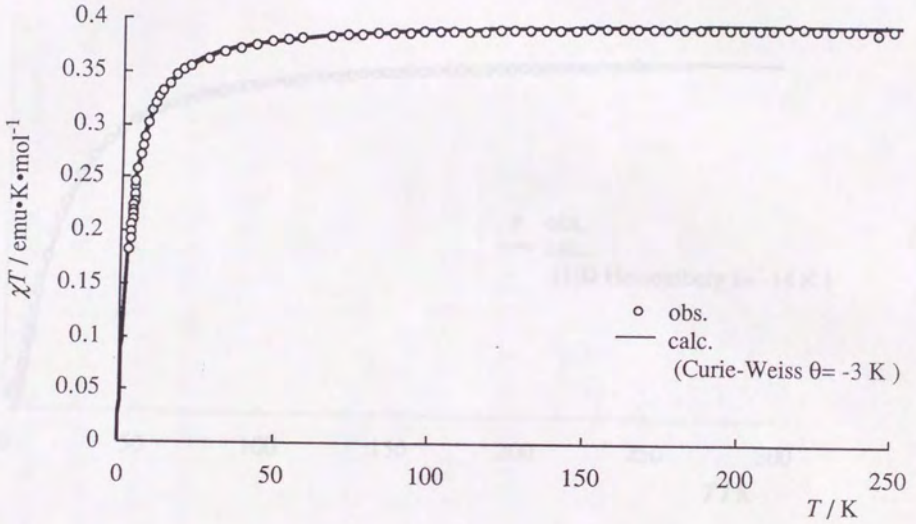

Figure III-6. χT-T plot of neutral **3**.

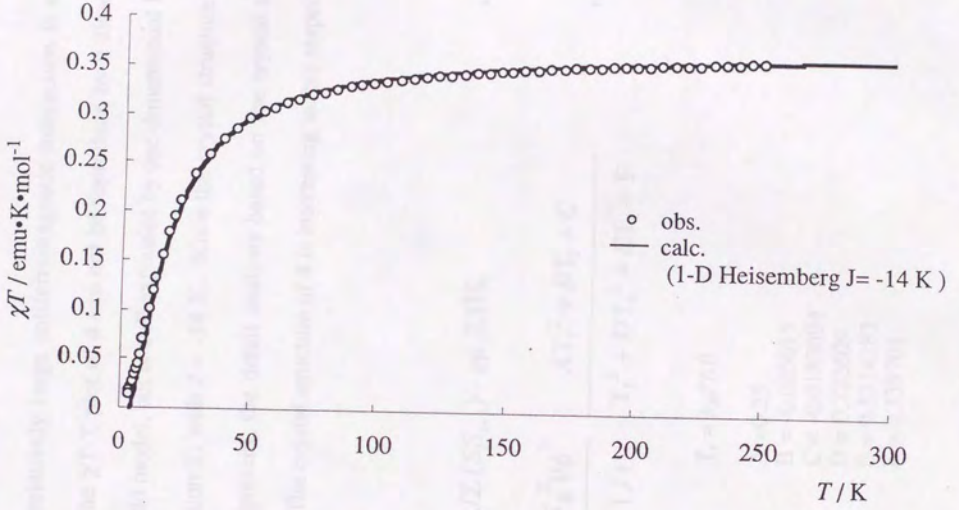

Figure III-7. χT-T plot of neutral **4**.

negligibly small.

Whereas relatively large antiferromagnetic interaction is expected in crystal **4**. The χT-T plot of **4** can not be reproduce by a dimer model or molecular field model, but is well explained by one-dimensional Heisemberg model (equation 2) with J = -14 K. Since the crystal structure of **4** is not available at present, the detail analysis based on the crystal structure is impossible. The crystal structure of **4** is interesting in this respect.

$$\boldsymbol{H} = 2J\Sigma (S_i S_{i+1}) - g\mu_\beta \Sigma \mathbf{H} S_i \qquad \cdots (1)$$

$$\chi = \frac{N_g{}^2 \mu_\beta{}^2}{|J|} \frac{A T_r{}^2 + B T_r + C}{T_r{}^3 + D T_r{}^2 + E T_r + F} \qquad \cdots (2)$$

where $T_r = k_B T/|J|$

A =0.25
B = -0.005015
C = -0.0187094
D = 0.722609
E = 0.5714283
F = 0.339701

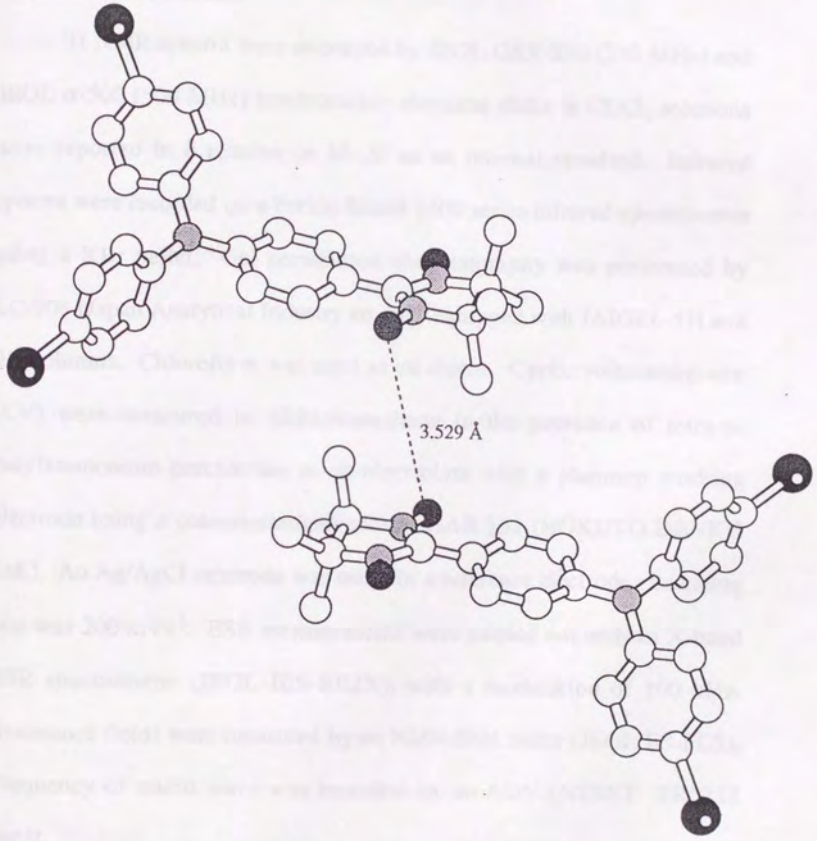

Figure III-8 O•••O contact in the crystal of neutral **3**

2-6. Experimental

1) General Procedures.

^{1}H NMR spectra were measured by JEOL GSX-270 (270 MHz) and JEOL α-500 (500 MHz) spectrometer, chemical shifts in $CDCl_3$ solutions were reported in δ relative to Me_4Si as an internal standard. Infrared spectra were recorded on a Perkin Elmer 1400 series infrared spectrometer using a KBr pellet. Gel permeation chromatgraphy was performed by LC-908 (Japan Analytical Industry co.,ltd.) equipped with JAIGEL-1H and 2H columns. Chloroform was used as an eluent. Cyclic voltammograms (CV) were measured in dichloromethane in the presence of tetra-n-butylammonium perchlorate as an electrolyte with a platinum working electrode using a potentiostat/galvanostat HAB 151 (HOKUTO DENKO Ltd.). An Ag/AgCl electrode was used for a reference electrode. Scanning rate was 200 mVs^{-1}. ESR measurements were carried out with an X-band ESR spectrometer (JEOL JES-RE2X), with a modulation of 100 kHz. Resonance fields were measured by an NMR field meter (JEOL ES-FC5). Frequency of micro wave was recorded by an ADVANTEST TR5212 meter.

2) Materials.

Formyl-TTF[24] (**10**), 2,3-dimethyl-2,3-bishydroxylaminobutan (**11**), 2,3-dimethyl-2,3-bishydroxylaminobutan sulfate[25], and tris(*p*-bromophenyl)-amine[26] were prepared according to the published procedures. Tetrahydrofuran (THF) and diethyl ether were distilled over sodium metal and benzophenone immediately prior to use. Benzene was distilled over sodium metal. Dimethylformamide (DMF) was distilled over CaH_2. All other reagents were used as purchased without further purification.

3) Preparations.

2-Tetrathiafulvalenyl-1,3-bishydroxy-imidazolidine (12): In a 50 ml round-bottomed flask, 0.30 g (1.29 mmol) of formyl-TTF (**10**), 0.39 g (2.64 mmol) of 2,3-dimethyl-2,3-bishydroxylaminobutane, 45 ml of pentane and 1.5 ml of methanol were added. To this suspension, 30 mg of 2,3-dimethyl-2,3-bishydroxylaminobutane sulfate and 30 mg of powdered zeolite was also added. The mixture was heated under reflux for 2 days under a N_2 atmosphere. The solvent was evaporated and $CHCl_3$ was added to the reaction mixture. The yellow precipitate was filtered and washed well with $CHCl_3$ and methanol. Among the residue, the insoluble parts to THF were collected. The solution was dried over $MgSO_4$, and the solvent was evaporated to give yellow powder; Yield 22 % (0.10 g, 0.28 mmol); ^{1}H-NMR (DMSO-d_6) δ = 0.98 (s, CH_3, 12H), 4.31 (s, CH, 1H), 6.66 (s,

C=CH, 1H), 6.69 (s, CH=CH, 2H), 8.07 (s, OH, 2H).

TTF-NN (2): To a stirred mixture of 0.10 g (0.28 mmol) of cyclic bishydroxylamine (**12**), 0.10 g of K_2CO_3 and anhydrous THF which was cooled at -30 °C, 1.30 g (5.44 mmol) of PbO_2 was added under a N_2 atmosphere. The color of the solution was turned into red immediately, then the mixture was stirred for ca. 10 minutes. The residue was removed filtration and the filtrate was evaporated under reduced pressure, and the crude product was column chromatographed on silicagel using 3:1 hexane - diethyl ether as an eluent at -30 °C. The red solution was collected and solvent was removed by evaporation to give red solid; m.p 77.9 °C (dec.); IR (KBr) 1461, 1559 cm^{-1} ($\nu_{C=C}$), 1422, 1378 cm^{-1} (ν_{NO}); MAS (FAB) $(M^+ +1)_{obs} = 360.06$, $M^+_{calc} = 359.00$.

4-Bis(*p*-bromophenyl)amino-benzaldehyde (14): To a solution of 5.00 g (10.4 mmol) of tris(p-bromophenyl)amine of anhydrous diethyl ether, 6.4 ml (10.4 mmol) of n-BuLi (15 % in n-Hex. d = 0.69) was added at -30 °C under a N_2 atmosphere. The mixture was warmed slowly to room temperature, then the mixture was stirred for 1 hour. To this mixture, 1.4 ml (31.2 mmol) of DMF was added at -10 °C with stirring. The mixture was stirred for 1 hour at room temperature and a drop of H_2O was added. The mixture was filtered by a phase separator and the filtrate was evaporated

under reduced pressure, and the residue was column chromatographed on silicagel using 1:1 hexane - $CHCl_3$ as an eluent. Crystallization from n-hexane solution gave pure crystals of **14**; Yield 58 % (2.60 g, 6.03 mmol); ^{1}H-NMR ($CHCl_3$) δ = 7.02 (d, Ar, 4H), 7.04 (d, Ar, 2H), 7.45 (d, Ar, 4H), 7.72 (d, Ar, 2H), 9.84 (s, CHO, 1H).

2-(4'-Bis(*p*-bromophenyl)aminophenyl)-1,3-bishydroxy-imidazolidine (15): In a 30 ml round-bottomed flask, 1.23 g (2.85 mmol) of formyl derivative (14) , 0.50 g (3.38 mmol) of 2,3-dimethyl-2,3-bishydroxylaminobutane, 0.05 g of 2,3-dimethyl-2,3-bishydroxylaminobutane sulfate, 12 ml of benzene and 2.5 ml of methanol were added. The mixture was heated under reflux for 1 day under a N_2 atmosphere. The colorless precipitates were filtered and washed with cold methanol; Yield 62 % (1.00 g, 1.78 mmol); ^{1}H-NMR (DMSO-d_6) δ = 1.05 (d, CH_3, 12H), 4.48 (s, CH, 1H), 6.91 (d, Ar, 4H), 7.02 (d, Ar, 2H), 7.43 (d, Ar, 2H), 7.45 (d, Ar, 4H), 7.78 (s, OH, 2H).

***p*-TPA-NN (3)**: To a mixture of 0.03 g (0.05 mmol) of cyclic hydroxylamine (**15**) and 3 ml of benzene, 0.10 g (0.42 mmol) of PbO_2 was added under a N_2 atmosphere. The resulting colored mixture was stirred for 1 hour. After filtration, the solvent was removed by evaporation. The crystalline residue was column chromatographed on silicagel using diethyl ether as an

eluent. The slow evaporation of diethyl ether solution give blue plate; IR (KBr) 1418, 1316 cm^{-1} (ν_{NO}); MAS $M^{+}_{obs} = 558$, $M^{+}_{calc} = 558$.

3-Diphenylamino-ethylbenzoate (17): In a 50 ml round-bottomed flask equipped an air-reflux condenser and a Dean-Stark trap, 1.77 g (10.5 mmol) of diphenylamine, 2.75 g (9.96 mmol) of *m*-iodo-ethylbenzoate, 1.4 g (10.0 mmol) of powdered K_2CO_3, 0.05 g (0.79 mmol) of Cu powder and 20 ml of nitrobenzene was added. The mixture was heated under reflux for 3 days. The solvent was removed by evaporation under reduced pressure (~ 5 mmHg). The reaction mixture was extracted with 200 ml of benzene. The extract was washed three times with 200 ml of water and once with 200 ml of saturated aqueous NaCl, and dried over $MgSO_4$. Benzene was evaporated to give crude **17**. The crude product was purified by column chromatography on silicagel using using 1:1 hexane - $CHCl_3$ as an eluent. The pale yellow plate recrystallized from ethanol; Yield 51 % (1.62 g, 5.09 mmol); ^{1}H-NMR ($CHCl_3$) δ = 1.34 ppm (t, 3H, CH_3), 4.32 (q, 2H, CH_2), 7.00 ~ 7.09 (m, Ar, 6H), 7.22 ~ 7.31 (m, Ar, 6H), 7.65 (m, Ar, 1H), 7.76 (m, Ar, 1H) .

***N,N*-Diphenylamino-3-hydroxymethyl-aniline (18)**: To an ice-cooled, stirred solution of ester **17** (0.43 g, 1.36 mmol) in dry diethyl ether (10 ml), 0.50 g (1.32 mmol) of $LiAlH_4$ was added in small portions under N_2

atmosphere and the mixture was refluxed for 30 minutes. After addition of ethylacetate (1 ml), water (10 ml) was added dropwise to the reaction mixture. The reaction mixture was filtered by a phase separator and the filtrate was evaporated under reduced pressure to give alcohol **18**. The product was used without further purification; Yield 100 % (0.38 g, 1.38 mmol); ^{1}H-NMR ($CHCl_3$) δ = 4.10 ppm (s, CH_2, 2H), 6.97 ~ 7.28 (m, Ar, 12H), 7.51 (m, Ar, 1H), 7.95 (m, Ar, 1H).

3-Diphenylamino-benzaldehyde (**19**): To a suspension of 0.52 g (2.41 mmol) of pyridinium chlorochromate (PCC) in dichloromethane (80 ml), 0.44 g (1.60 mmol) of **18** (crude) in dichloromethane (20 ml) was added and the mixture was stirred at room temperature for 3 hours. To the reaction mixture, diethyl ether was added and the precipitates were filtered off through celite. The filtrate was evaporated and the residue was purified by silicagel column chromatography with 1:1 hexane-$CHCl_3$ as an eluent, giving **19**. The aldehyde was used without further purification; Yield 58 % (0.25 g, 0.92 mmol); ^{1}H-NMR ($CHCl_3$) δ = 7.04 ~ 7.57 ppm (m, Ar, 14H), 9.89 (s, CHO, 1H).

3-Bis(*p*-bromophenyl)amino-benzaldehyde (**20**): To a solution of 0.25 g (0.92 mmol) of aldehyde **19** in $CHCl_3$ (5 ml), a solution of 0.88 g (1.83 mmol) of n-$Bu_4N{\bullet}Br_3$ in $CHCl_3$ (5 ml) was added. The mixture was

stirred for 3 hours at room temperature under a N_2 atmosphere. To the reaction mixture, $NaHSO_3$ aq was added and was filtered by a phase separator. The filtrate was evaporated and the residue was purified by recrystallization from n-hexane to give pale yellow solid; Yield 48 % (0.19 g, 0.44 mmol); ^{1}H-NMR ($CHCl_3$) δ = 6.95 ppm (d, Ar, 4H), 7.28 ~ 7.32 (m, Ar, 2H), 7.38 (d, Ar, 4H), 7.50 ~ 7.53 (m, Ar, 2H), 9.90 (s, CHO, 1H).

2-(3'-Bis(*p*-bromophenyl)aminophenyl)-1,3-bishydroxy-imidazolidine (21): In a 30 ml round-bottomed flask, 0.22 g (0.51 mmol) of aldehyde **20** , 0.12 g (0.81 mmol) of 2,3-dimethyl-2,3-bishydroxylaminobutane, 0.01 g of 2,3-dimethyl-2,3-bishydroxylaminobutane sulfate, 5 ml of benzene and 1 ml of methanol were added. The mixture was stirred at 50°C for over night under a N_2 atmosphere. The colorless precipitates were filtered and washed with cold methanol. The cyclic hydroxylamine was used without further purification.

***m*-TPA-NN (4)**: To a mixture of 0.21 g of precursor **21** and 10 ml of benzene, 2.10 g of PbO_2 was added under a N_2 atmosphere. The resulting colored mixture was stirred for 30 minutes. After filtration through celite, the solvent was removed by evaporation. The residue was purified by column chromatography on silicagel using diethyl ether as an eluent. The solvent was removed by evaporation to give blue powder **4**; IR (KBr)

4. Exchange Interaction of One-Electron Oxidation State of Open-Shell Donors

4-1. ESR Spectrum and Ground State Spin Multiplicity of $(TTF\text{-}NN)^{+\bullet}$

The open-shell donor **2** was oxidized by excess I_2 in 2-methyltetrahydrofuran (MTHF) to afford a green solution. The ESR spectrum of the oxidized species in a frozen matrix of MTHF at 100 K showed a set of signals due to the triplet species (Figure IV-1) along with a signal (g = 4.030) of $\Delta m_s = 2$ in a half-field region. Zero-field splitting parameters and anisotropic g-values of the triplet species were determined by computational simulation (Figure IV-1) to be $D = 0.0214$, $E = 0.0022$ cm^{-1} and $g_x = 2.0111$, $g_y = 2.0094$, $g_z = 2.0031$, respectively. These parameters indicate that the obtained fine structure is due to the cation biradical $\mathbf{2}^{+\bullet}$. The g-value of $\mathbf{2}^{+\bullet}$ ($g = 1/3\ (g_x + g_y + g_z)$ = 2.0079) corresponds to the average between the unsubstituted nitronyl nitroxide radical NN-H[28] (**22**) (g = 2.0063) and TTF cation radical[29] (g = 2.0084).

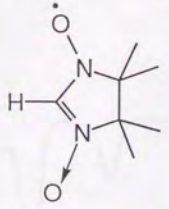

22

Temperature dependence of the signal intensity in THF glass was measured in the temperature range of 50 ~ 150 K (Figure IV-2). The plot reveals that the triplet signals are derived from thermally populated species and that two spins interact antiferromagnetically. Using a S–T model, the

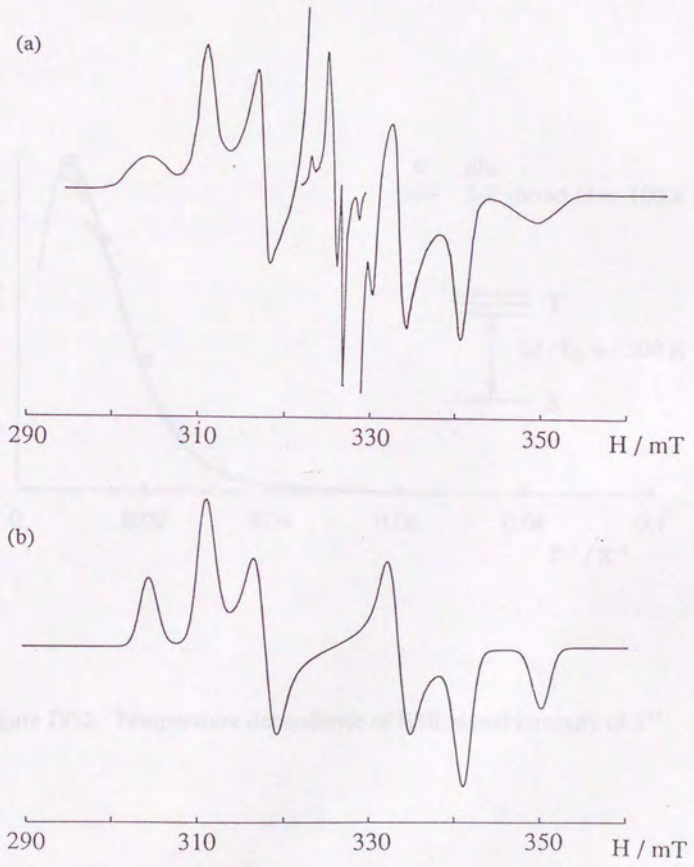

Figure IV-1. ESR spectrum of $2^{+\bullet}$ in MTHF glass.
(a) observed spectrum (central lines are due to the neutral species)
(b) simulated spectrum

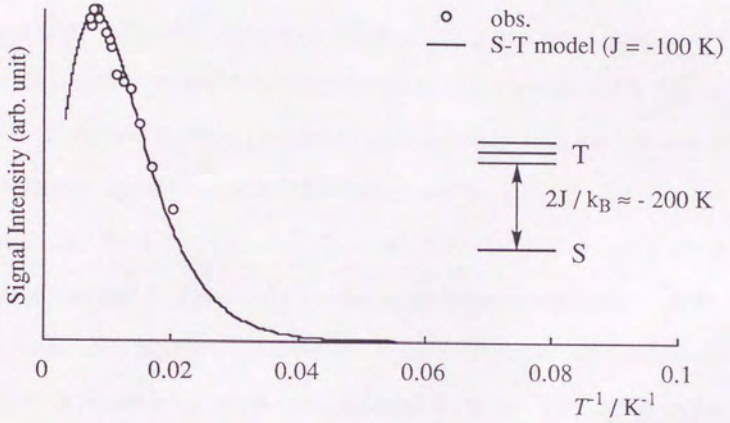

Figure IV-2. Temperature dependence of ESR signal intensity of $\mathbf{2}^{+\bullet}$

exchange interaction ($|J|/k_B$) was estimated to be about 100 K (Figure IV-2).

4-2. ESR Spectrum and Ground State Spin Multiplicity of (*p*-TPA-NN)$^{+\bullet}$ and (*m*-TPA-NN)$^{+\bullet}$

The open-shell donors **3** and **4** were oxidized by excess I_2 in MTHF to afford green solutions of the cation biradical. ESR spectra of the oxidized species in matrix showed fine structures due to triplet species at 6 K (Figure IV-3). Zero-field splitting parameters were estimated from the line shapes of the triplet signal, $D = 0.0261$, $E = 0.0019$ cm^{-1} for **3** and $D = 0.0254$, $E = 0.0023$ cm^{-1} for **4**, respectively. These relatively large D values indicate that the obtained fine structures are due to the cation biradicals **3**$^{+\bullet}$ and **4**$^{+\bullet}$. The exchange interactions between two spins in **3**$^{+\bullet}$ and **4**$^{+\bullet}$ were examined cautiously by the temperature dependence of the triplet ESR signals in the temperature range of 6 ~ 110 K. The obtained Curie plots indicate that the triplet signals for both **3**$^{+\bullet}$ and **4**$^{+\bullet}$ are assignable to the ground state triplet species (Figure IV-4).

The Curie plot suggests that these species exist as ground state triplets or have thermally accessible triplet states. In the latter case, ESR spectra should show additional resonance lines due to the S-T mixing at cryogenic temperature. Since the spectral pattern does not change even very low temperature, this possibility may be excluded.

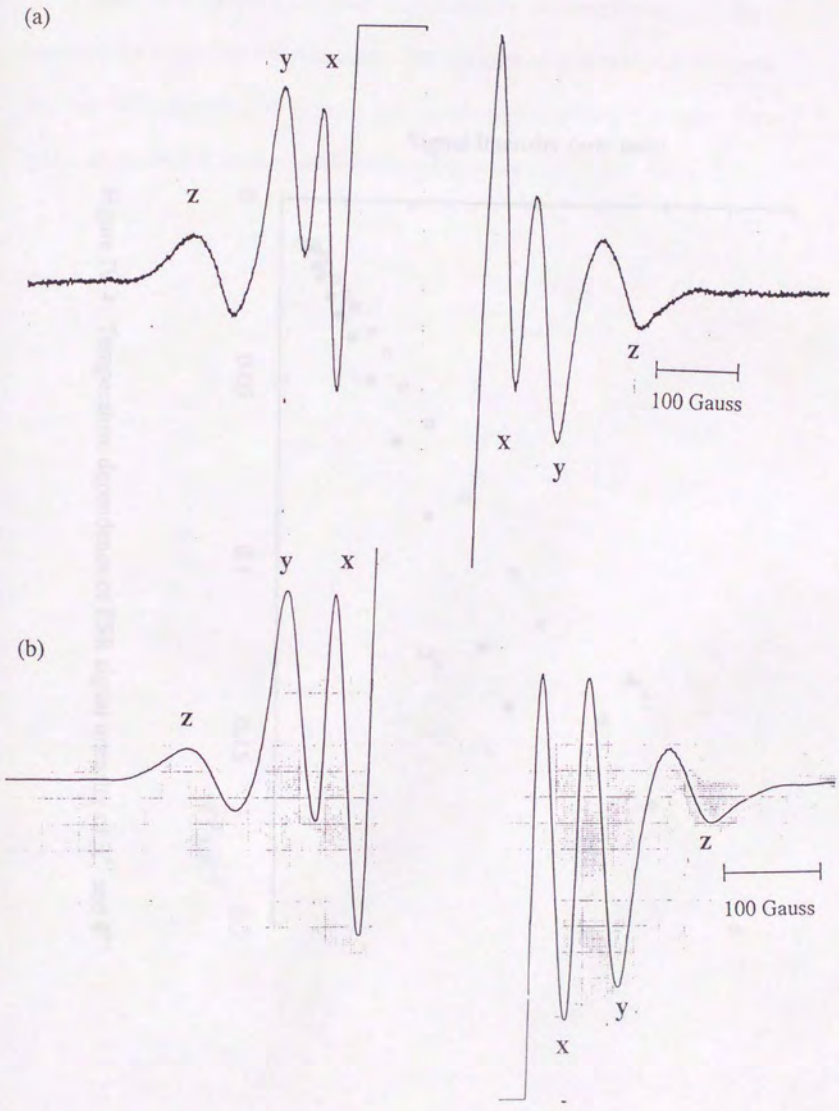

Figure IV-3. (a) ESR spectrum of $3^{+\bullet}$ in MTHF glass.
(b) ESR spectrum of $4^{+\bullet}$ in MTHF glass.

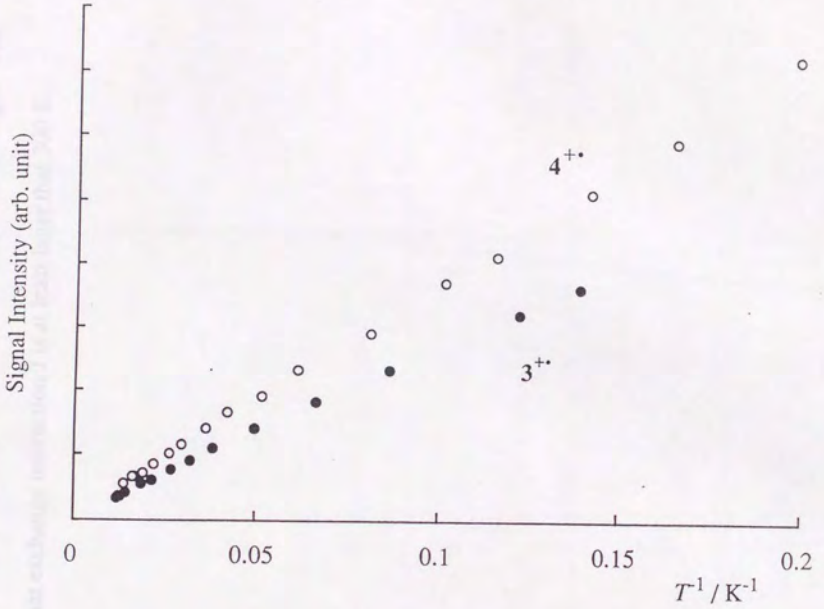

Figure IV-4. Temperature dependence of ESR signal intensity of $\mathbf{3}^{+\bullet}$ and $\mathbf{4}^{+\bullet}$

Figure IV-5 shows χT-T plots calculated by varying the energy gaps between the singlet and triplet states. The experimental Curie plot does not deviate from the straight line in the measured temperature range. The result suggests that exchange interaction J is at least lager that 300 K.

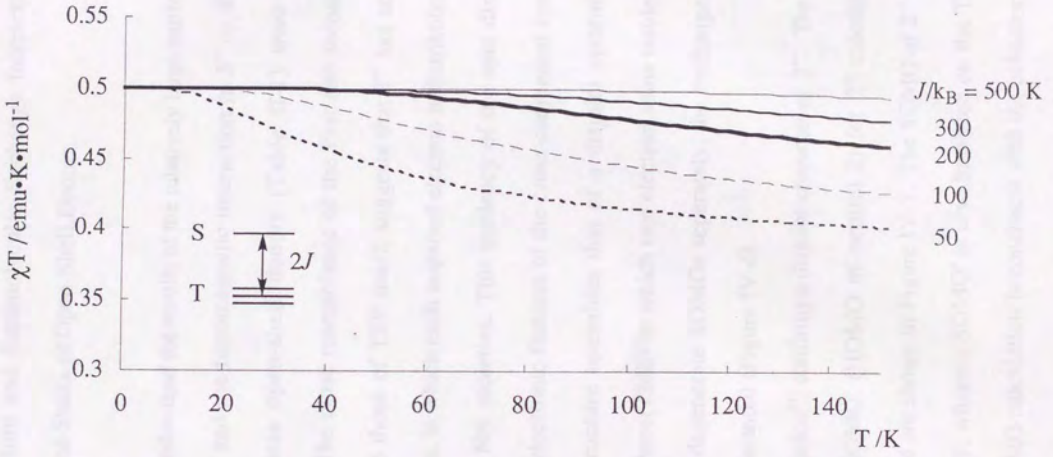

Figure IV-5 χT-T plots calculated by varying energy gaps between singlet and triplet states.

4-3. MO Structure and Intramolecular Exchange Interaction of One-Electron Oxidation States of Open-Shell Donors.

In order to understand the results of the relatively large antiferromagnetic interaction in $\mathbf{2}^{+\cdot}$ and the ferromagnetic interaction in $\mathbf{3}^{+\cdot}$ or $\mathbf{4}^{+\cdot}$, oxidation potentials of these open-shell donors (Table II-1) were taken into consideration. The close resemblance of the first and second oxidation potentials of **2** to those of TTF itself, suggests that $\mathbf{2}^{+\cdot}$ has an open-shell biradical structure, in which each unpaired electron is distributed separately on the TTF and NN moieties. This tendency of the spin distribution is reflection of the electronic features of the cross-conjugated system. Since the electronic structure resembles that of a disjoint system[30], such as tetramethyleneethane(TME) in which two electron spins reside in separate allyl moieties of degenerate SOMOs separately, the exchange interaction should not be substantial (Figure IV-6).

A MO calculation[31] confirms a disjoint-character of $\mathbf{2}^{+\cdot}$. The coefficients of SOMO and SOMO' (HOMO of neutral **2**) for $\mathbf{2}^{+\cdot}$ calculated by the PM3/UHF method are shown in Figure IV-7. The SOMO of $\mathbf{2}^{+\cdot}$ is localized on the NN moiety, whereas SOMO' is also localized on the TTF moiety. The result of the MO calculation is consistent with the oxidation potentials.

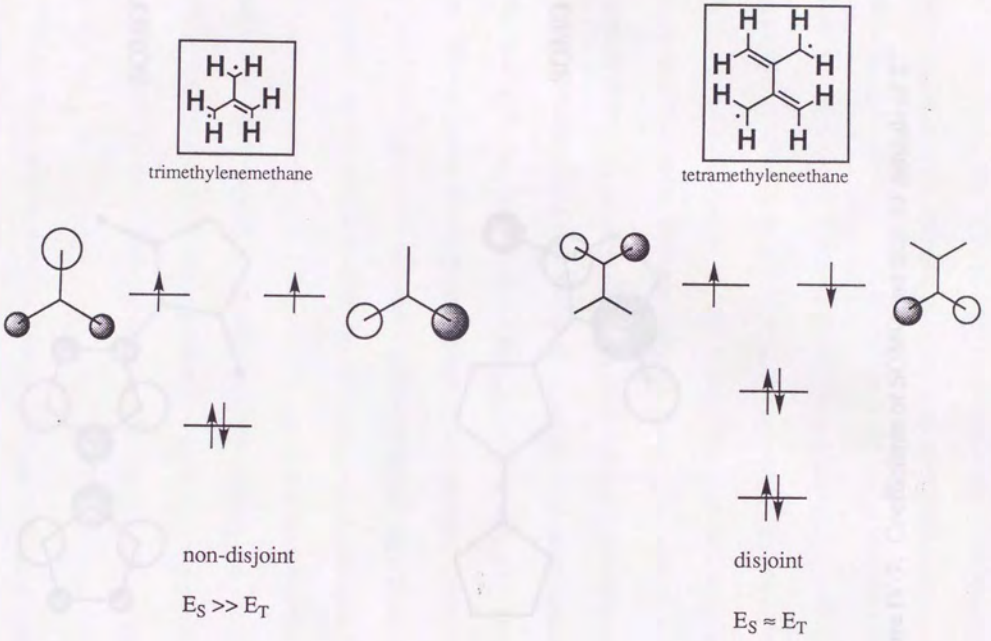

Figure IV-6 Trimethylenemethane and tetramethyleneethane.

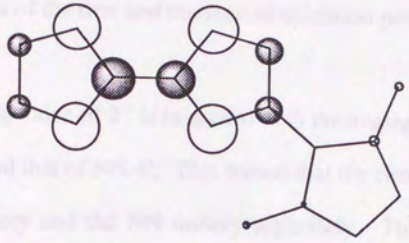

SOMO'

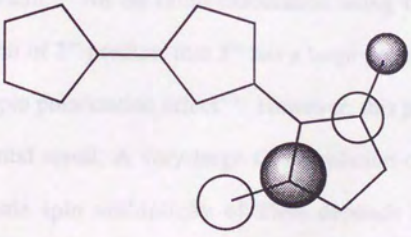

SOMO

Figure IV-7. Coefficients of SOMO and SOMO' orbitals of $2^{+\bullet}$

Because the HOMO of **2** is localized on the TTF moiety, the energy level of HOMO of **2** is almost the same as that of TTF itself. This suggests that the values of the first and the second oxidation potentials of **2** resemble that of TTF.

The g-value of $\mathbf{2}^{2+}$ is in accord with the average between the g-value of TTF+• and that of NN-H. This means that the two unpaired spins reside on TTF moiety and the NN moiety separately. The tendency is consistent with the above interpretation.

In the cation biradical $\mathbf{2}^{2+}$, relatively large antiferromagnetic interaction was observed. The disjoint character predicts small exchange interaction in the system. An *ab initio* calculation using the model system of the planar form of $\mathbf{2}^{2+}$ predicts that $\mathbf{2}^{2+}$ has a large positive exchange interaction due to a spin polarization effect[32]. However, this prediction contradicts the experimental result. A very large CI calculation on TME reveals that the ground state spin multiplicity of TME depends heavily on the dihedral angle between two allyl moieties[33]. Thus in order to examine the ground state multiplicity of $\mathbf{2}^{2+}$ theoretically, a CI calculation of the similar level may be required. Besides it is suggested that some interaction may operate in cation biradical $\mathbf{2}^{2+}$: for instance, an intramolecular CT interaction and/or a through-space interaction between the cation radical of TTF moiety and the NN moiety. The former interaction stabilizes the S_3 state in the

Figure III-1. Additionally, the S_1 state may be stabilized by CI interaction between S_1 and S_2 (and/or S_3) state. After all, the spin system of this cation biradical is characterized by the small $K_{ss'}$ because of the non-disjoint character. Thus that the T_0 state is not stabilized enough to become the ground state.

In sharp contrast with the case of **2**, the first oxidation potential of **3** or **4** is found to be shifted to the lower side by 0.42, 0.36 V, respectively, compared with that of tris(*p*-bromophenyl)amine. This result suggests that the energy level of the HOMO of **3** or **4** is raised due to the interaction between donor and NN moieties (Figure IV-8).

The interaction may be expained if the perturbation molecular orbital theory is applied to the open-shell donor, which consists of the donor and radical moieties. The *homo* of the donor moiety interacts with *nhomo* of the NN moiety, pushing the energy level of HOMO of the open-shell donor higher.

The MO calculation supports the above interpretation. The coefficients of SOMO and SOMO' (HOMO of neutral open-shell donor) for both $\mathbf{3}^{+\bullet}$ and $\mathbf{4}^{+\bullet}$ calculated by the PM3/UHF method are shown in Figure IV-9. While the SOMO of $\mathbf{3}^{+\bullet}$ is localized on the NN moiety, the SOMO' distributes over the entire molecule framework. This tendency is caused by the *homo-nhomo* interaction aforementioned.

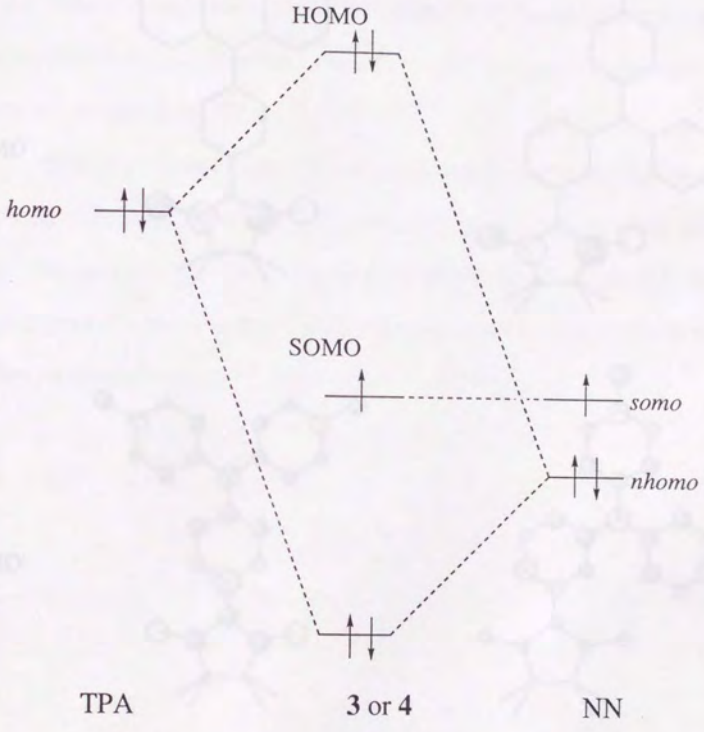

Figure IV-8. Schematic drawing of the electronic configuration of **3** or **4**

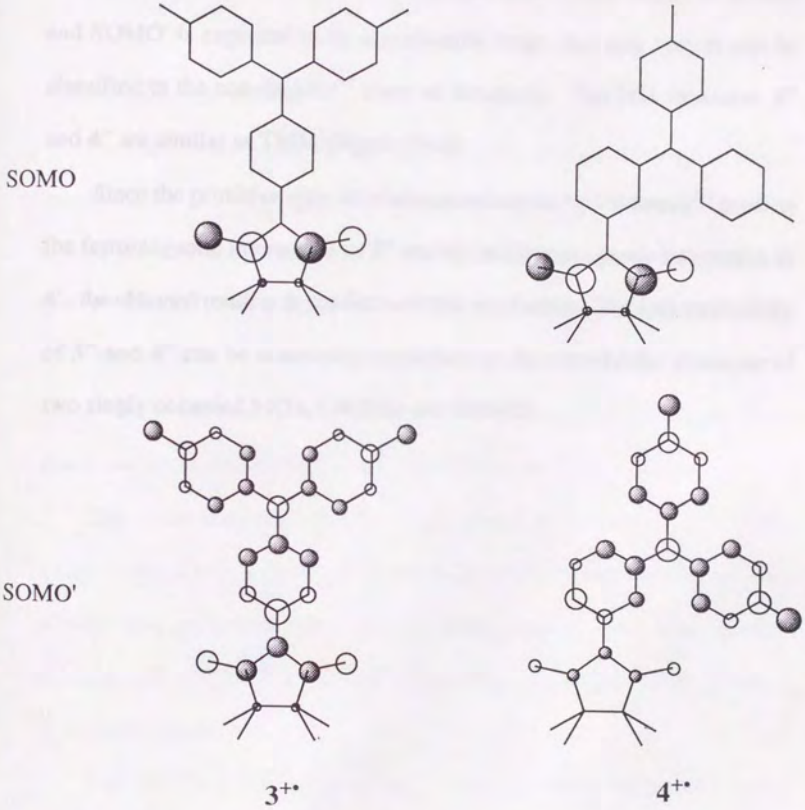

Figure IV-9. Coefficients of SOMO and SOMO' orbitals of $3^{+\bullet}$ and $4^{+\bullet}$

The situation of $\mathbf{4}^{+\cdot}$ is exactly similar to the para-derivative. Thus the exchange interaction between two electron spins which reside in SOMO and SOMO' is expected to be significantly large: this spin system can be classified in the non-disjoint[30] class of biradicals. The MO structures $\mathbf{3}^{+\cdot}$ and $\mathbf{4}^{+\cdot}$ are similar as TMM (Figure IV-6).

Since the primitive spin alternation mechanism by VB theory[34] predicts the ferromagnetic interaction in $\mathbf{3}^{+\cdot}$ and the antiferromagnetic interaction in $\mathbf{4}^{+\cdot}$, the obtained result is in conflict with this mechanism. The spin multiplicity of $\mathbf{3}^{+\cdot}$ and $\mathbf{4}^{+\cdot}$ can be reasonably explained by the non-disjoint character of two singly occupied MO's, (SOMO and SOMO').

4-4. Experimental

1) ESR measurements

Commercially supplied 2-methyltetrahydrofuran (MTHF) was purified by distillation over Na. The ESR measurements were carried out with an X-band ESR spectrometer (JEOL JES-RE2X), 100 kHz modulation, equipped with a cryostat (Air Products LTR-5500). The temperature was measured by using an Au-Fe-Chromel thermocouple. Resonance fields were measured by an NMR field meter (JEOL ES-FC5). Frequency of the micro wave was recorded by an ADVANTEST TR5212 meter.

The donor molecule **2**, **3** or **4** was dissolved in MTHF in an ESR sample tube, and oxidized by excess I_2 to afford a green solution. The solution was immediately degassed by three times of freeze-thaw cycles. A triplet ESR spectra of $\mathbf{2}^{+\cdot}$, $\mathbf{3}^{+\cdot}$ and $\mathbf{4}^{+\cdot}$ were obtained in glasses at 110 K, 6 K and 6 K, respectively.

The zero-field splitting parameters and anisotropic g-values of $\mathbf{2}^{+\cdot}$ were determined by spectrum simulation and the zero-field splitting parameters of $\mathbf{3}^{+\cdot}$ and $\mathbf{4}^{+\cdot}$ were obtained by spectrum shapes.

2) Simulation of ESR spectra

Simulation of ESR spectra was carried out for randomly oriented triplet species, of which ESR absorption lines reproduced by the fine-structure spin Hamiltonian with the spin multiplicity of $2S + 1 = 3$.

$$\boldsymbol{H} = \beta(\mathbf{S}\cdot\mathbf{g}\cdot\mathbf{H}) + D[S_z^2 - S(S+1)/3] + E(S_X^2 - S_Y^2)$$

Resonance fields and transition probabilities were obtained on the basis of the above spin Hamiltonian using the third order perturbation theory. The best fit Hamiltonian parameters were obtained to be $|D| = 0.0214$, $|E| = 0.0022$ cm^{-1}, $g_x = 2.0111$, $g_y = 2.0094$ and $g_z = 2.0031$ for $\mathbf{2}^{+\cdot}$.

3) MO calculations

A calculations was carried out on the triplet state of $\mathbf{2}^{+\cdot}$, $\mathbf{3}^{+\cdot}$ or $\mathbf{4}^{+\cdot}$ with the PM3 Hamiltonian and a UHF method on the IBM RISC System 6000 using MOPAC Ver. 6.00 (QCPE No. 445) program.

5. Summary

One-electron oxidation state of the open-shall donor is the novel triplet spin system which have non-degenerated SOMOs. There are two kind of spins. They are the p-delocalized spin which resides at the singly oxidized donor moiety, and the localized spin at the NN moiety, and the exchange interaction exists between these two spins. In addition, both *para-* and *meta-* substituted compounds ($\mathbf{3}^{+\cdot}$, $\mathbf{4}^{+\cdot}$), have ferromagnetic interaction. The primitive spin alternation can not explain this mechanism. The conflict may be caused by the skeleton of triphenyl amine (TPA) which has the hetero atom. The feature of MO of the cation radical of TPA is different from benzyl radical, which is classified as an odd-alternant hydrocarbon as shown in Figure V-1. In the benzyl radical, coefficients of SOMO are localized at ortho- and para- positions, but in the cation radical of aniline, carbon atoms of the meta-position have coefficients to some extent. Thus, the primitive spin alternation mechanism is not appriable to explain the spin system which contains hetero atoms.

The requirement of achieving the triplet ground state species based on the singly oxidized open-shell donor can be summarized as follows. 1) The orbital energy of HOMO is higher that of SOMO which is localized at radical moiety. 2) In the one-electron oxidation state, two SOMOs (SOMO and SOMO') should exist. In other word, one-electron oxidation state of

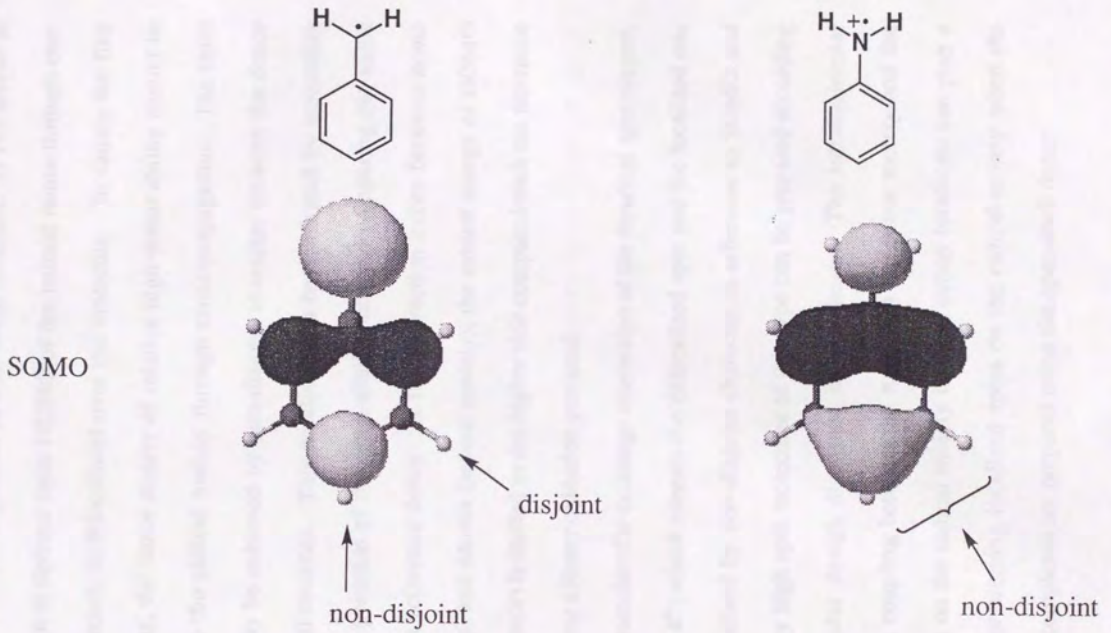

Figure V-1 Coefficients of SOMO of benzyl and aniline$^{+\bullet}$

the open-shell donor is expressed as a biradical structure. 3) The orbital of SOMO', which is derived from HOMO of the neutral donor through one-electron oxidation, is delocalized over the molecule. To satisfy the first two conditions, the donor moiety of relative high donor ability should be substituted to the radical moiety through cross-conjugation. The third condition may be achieved by non-disjoint character between the donor and the radical moieties. This condition can be confirmed by measuring the oxidation potential of the open-shell donor and comparing the value with that of a reference donor. If the interaction exists between *homo* (donor moiety) and *nhomo* (radical moiety), the orbital energy of HOMO (open-shell donor) is shifted to the higher side compared with the reference donor exhibiting a lower oxidation potential.

The intramolecular exchange interaction of the biradical spin system, such as $\mathbf{3}^{+\cdot}$ or $\mathbf{4}^{+\cdot}$, which contain the delocalized spin and the localized one is well rationalized by non-disjoint character in reference to SOMO and SOMO'. Many high spin molecules of this type can be prepared according to the molecular design discussed in this thesis. The intramolecular ferromagnetic coupling between the π spin on the donor moiety and the localized spin on the radical moiety in these cation biradicals can play a crucial role for aligning localized spins on the radical moiety when the mixed-valent complexes are prepared using the open-shell donor.

Basing upon the guiding principle of discussed in this thesis, novel triplet species derived from open-shell donors, have been prepared and the ground state multiplicity of the singly oxidized states of these donors have been examined. Although donor ability of TTF moiety in **2** is reasonably high to manifest a conductive property when they are partially oxidized and assembled, the exchange interaction between localized spin and the conducting electron has a negative sign. This suggests that **2** is expected to be a constituent of organic Kondo system[2b),35)]. Moreover, **2** is the first example of open-shell donor whose intramolecular exchange interaction (J) between donor moiety and radical moiety in the one-electron oxidation state is estimated. Whereas singly oxidized donors, $\mathbf{3}^{+\cdot}$ and $\mathbf{4}^{+\cdot}$, is found to exhibit positive exchange interaction. The precise molecule design based on the guiding principle discussed here should lead to an organic ferromagnetic metal.

References

1. (a) M. Kinoshita, P. Turek, M. Tamura, K. Nozawa, D. Shiomi, Y. Nakazawa, M. Ishikawa, M. Takahashi, K. Awaga, T. Inabe, Y. Maruyama, *Chem. Lett.*, **1991**, 1225. (b) R.Chiarelli, M. A. Novak, A. Rassat, J. L. Tholence, *Nature*, **363**, 147 (1993). (c) P-M. Allemand, K. C. Khemani, A. Koch, F. Wudl, K. Holczer, S. Donovan, G. Grüner, J. D. Thompson, *Science*, **253**, 301 (1991). (d) T. Nogami, K. Tomioka, T. Ishida, H. Yoshikawa, M. Yasui, F. Iwasaki, H. Iwamura, N. Takeda, M. Ishikawa, *Chem. Lett.*, **1994**, 29. (e) T. Sugawara, M. M. Matsushita, A. Izuoka, N. Wada, N.Takeda, M. Ishikawa, *J. Chem. Soc. Chem. Commun.*, **1994**, 1723.
2. (a) 近角聰信著, "強磁性体の物理", 裳華房 (1978). (b) 金森順次郎著, "磁性", 培風館 (1969). (c) 守谷享, 高橋慶紀, 科学, 54, 26 (1984). (d) E. C. Stoner, *Proc. Roy. Soc.*, **A154**, 656 (1936). (e) E. C. Stoner, *Proc. Roy. Soc.*, **A165,** 372 (1938). (f) E. C. Stoner, *Proc. Roy. Soc.*, **A169**, 339 (1939). (g) G. C. Fletcher, E. P. Wohlfarth, *Phil. Mag.*, **42**, 106 (1951). (h) J. C. Phillips, L. F. Mattheiss, *Phys. Rev. Lett.*, **11**, 556 (1963). (i) J. Yamashita, M. Fukuchi, S. Wakoh, *J. Phys. Soc. Jpn.*, **18**, 999 (1963). (j) S. Asano, J. Yamashita, *Prog. Theor. Phys.*, **49**, 373 (1972). (k) 和光信也, 山下次郎, 日本物理学会誌, 22, 3 (1967).
3. (a) M. A. Ruderman, C. Kittel, *Phys. Rev.*, **96**, 99 (1954). (b) T. Kasuya,

Prog. Theor. Phys., **16**, 45 (1956). (c) K. Yoshida, *Phys. Rev.* **106**, 893 (1957).

4. (a) G. H. Jonker, J. H. Van Santen, *Physica*, **16**, 337 (1950). (b) J. H. Van Santen, G. H. Jonker, *Physica*, **16**, 599 (1950).
5. C. Zener, *Phys. Rev.*, **82**, 403 (1951).
6. (a) A. Izuoka, R. Kumai, T. Tachikawa, T. Sugawara, *Mol. Cryst. Liq. Cryst.*, **218**, 213 (1992). (b) E. Dormann, M. J. Nowak, K. A. Williams, R. O. Angus Jr., F. Wudl, *J. Am. Chem. Soc.*, **109**, 2594 (1987).
7. (a) Y. Teki, T. Takui, K. Itoh, H. Iwamura, K. Kobayashi, *J. Am. Chem. Soc.*, **105**, 3722 (1983). (b) T. Sugawara, S. Bandow, K. Kimura, H. Iwamura, K. Itho, *ibid.*, **106**, 6449 (1984). (c) T. Sugawara, S. Bandow, K. Kimura, H. Iwamura, K. Itho, *ibid.*, **108**, 368 (1986). (d) N. Nakamura, K. Inoue, H. Iwamura, *Angew. Chem. Int. Ed. Engl.*, **32**, 872 (1993). (e) A. Rajca, S. Utamapanya, *J. Am. Chem. Soc.*, **115**, 2396, (1993). (f) J. Veciana, C. Rovira, M. I. Crespo, O. Armet, V. M. Domingo, F. Palacio, *J. Am. Chem. Soc.*, **113**, 2552 (1991). (g) A. Rajca, S. Rajca, R. Padmakumar, *Angew. Chem. Int. Ed. Engl.*, **33**, 2091 (1994).
8. E. Dormann, M. J. Nowak, K. A. Williams, R. O. Angus Jr., F. Wudl, *J. Am. Chem. Soc.*, **109**, 2594 (1987).
9. T. J. LePage, R. Breslow, *J. Am. Chem. Soc.*, **109**, 6412 (1987).
10. (a) A. Izuoka, R. Kumai, T. Sugawara, *Chem. Lett.*, **1992**, 285. (b) A.

Izuoka, R. Kumai, T. Tachikawa, T. Sugawara, *Mol. Cryst. Liq. Cryst.*, **218**, 213 (1992).

11. 明石康一, 工位武治, 木下隆正, 伊藤公一, 分子構造総合討論会 要旨集, 2C09 (1985).

12. (a) K. Bechgaard, K. Lerstrup, M. Jφrgensen, I. Johannsen, and J. Christensen, "The Physics and Chemistry of Organic Superconductors", Berlin, Springer-Verlag (1990), p.349. (b) K. Lerstrup, M. Jφrgensen, I. Johannsen, and K. Bechgaard, *ibid.*, p.383. (c) K. Bechgaard, K. Lerstrup, M. Jφrgensen, I. Johannsen, J. Christensen, and J. Larsen, *Mol. Cryst. Liq. Cryst.*, **181,** 161 (1990). (d) G. Rindorf, N. Thorup, K. Lerstrup, and K. Bechgaard, *Acta Crystallogr., Sect C*, **46**, 695 (1990). (e) M. L. Kaplan, R. C. Haddon, and F. Wudl, *J. Chem. Soc., Chem. Commun.*, **1977**, 388. (f) H. Tatemitsu, E. Nishikawa, Y. Sakata, and S. Misumi, *Synth. Metals*, **19**, 565 (1987). (g) J. Ippen, C. Tao-pen, B. Starker, D. Schweitzer, and H. A. Staab, *Angew. Chem., Int. Ed. Engl.*, **19**, 67 (1980). (h) T. Otsubo and F. Ogura, *Bull. Chem. Soc. Jpn.*, **58**, 1343 (1985). (i) F. Bertho-Thoraval, A. Robert, A. Souizi, K. Boubekeur, and P. Batail, *J. Chem. Soc., Chem. Commun.*, **1991**, 843. (j) M. Mizutani, K. Tanaka, K. Ikeda, K. Kawabata, *Synth. Met.*, **46**, 201 (1992). (k) M. Adam, V. Enkelmann, H. Räder, J. Röhrich, K. Müllen, Angew. Chem. Int. Ed. Engl., 31, 309 (1992). (l) M. Jφrgensen, K. Lerstrup, K. Bechgaard, *J. Org. Chem.*, **56**, 5684 (1991).

(m) M. R. Bryce, G. Cooke, A. S. Dhindsa, D. J. Ando, M. B. Hursthouse, *Tetrahedron Lett.*, **33**, 1783 (1992). (n) J. Becher, T. K. Hansen, N. Malhotra, G. Bojesen, S. Bowadt, K. S. Varma, B. Girmay, J. D. Kilburn, A. E. Underhill, *J. Chem. Soc. Prekin Trans.*, **1990**, 175. (o) T. Tachikawa, A. Izuoka, R. Kumai, T. Sugawara, Y. Sugawara, *Solid State Commun.*, **82**, 19 (1992).

13. M. T. Jones and D. B. Chesnut, *J. Chem. Phys.*, **38**, 1311 (1963).
14. G. Steimrcke, H. Sieler, R. Kirmse, E. Hoyer, *Phosphorus and Sulfur*, **7**, 49 (1979).
15. K. S. Varma, A. Bury, N. J. Harris, A. E. Underhill, *Synthesis*, **September 1987**, 837 (1987).
16. (a) T. Sugano, T. Fukasawa, M. Kinoshita, *Synth. Metals*, **41-43**, 3281 (1991). (b) T. Sugimoto, S. Yamaga, M. Nakai, M. Tsujii, H. Nakatsuji, N. Hosoito, *Chem. Lett.*, **1993**, 1817. (c) T. Ishida, K. Tomioka, T. Nogami, K. Yamaguchi, W. Mori, Y. Shirota, *Mol. Cryst. Liq. Cryst.*, **232**, 99 (1993).
17. (a) R. A. Moss, M. Jones Jr., "Carbenes" chapter 6, Wiley-Interscience, New York (1975). (b) W. Kirmse, "Carbene Chemistry" chapter 5, Academic Press, New York (1971)
18. W. Lwowski, "Nitrenes" chapter 2, Wiley-Interscience, New York (1970).
19. W. T. Borden, *Mol. Cryst. Liq. Cryst.* **232**, 195 (1993) and references

cited therein.

20. (a) B. B. Wright, M.S. Platz, M. S. *J. Am. Chem. Soc.*, **105**, 628 (1983). (b) S. Kato, K. Morokuma, D. Feller, E. R. Davidson, W. T. Borden, *J. Am. Chem. Soc.*, **105**, 1791 (1983).

21. (a) D. A.Dougherty, S. Joshuajacobs, S. K. Silverman, M. M. Murray, D. A. Shultz, S. P. West Jr., J. A. Clites, *Mol. Cryst. Liq. Cryst.* **232**, 289 (1993). (b) K. Yoshizawa, M. Hatanaka, A. Ito, K. Tanaka, T. Yamabe, *Mol. Cryst. Liq. Cryst.*, **232**, 323 (1993). (c) H. Tukada, *Mol. Cryst. Liq. Cryst.*, **233**, 9 (1993). (d) M. Matsushita, T. Nakamura, T. Momose, T. Shida, Y. Teki, T. Takui, T. Kinoshita, K. Itoh, *J. Am. Chem. Soc.*, **114**, 7470 (1992). (e) M. Matsushita, T. Nakamura, T. Momose, T. Shida, Y. Teki, T. Takui, T. Kinoshita, K. Itoh, *Bull. Chem. Soc. Jpn.*, **66**, 1333 (1993). (f) H. Mizouchi, A. Ikawa, H. Fukutome, *Mol. Cryst. Liq. Cryst.*, **233**, 127 (1993). (g) F. Wudl, P.-M. Allemand, P. Delhaes, Z. Soos, K. Hinkelmann, *Mol. Cryst. Liq. Cryst.*, **171**, 179 (1989). (h) J. S. Miller, D. A. Dixon, J. C. Calabrese, C. Vazquez, P. J. Krusic, M. D. Ward, E. Wasserman, R. L. Harlow, *J. Am. Chem. Soc.*, **112**, 381 (1990). (i) T. J. LePage, R. Breslow, R. *J. Am Chem. Soc.*, **109**, 6412 (1987). (j) E. Dormann, M. J. Nowak, K. A. Williams, R. O. Angus Jr., F. Wudl, *J. Am. Chem. Soc.*, **109**, 2594 (1987). (k) J. B. Torrance, S. Oostra, A. Nazzal, *Synth. Metals*, **19**, 709

(1987).

22. N. J. Turro, "Modern Molecular Photochemistry" chapter 2, The Benjamin/Cummings: California (1978).

23. R. Kumai, M. M. Matsushita, A. Izuoka, T. Sugawara, *J. Am. Chem. Soc.*, **116**, 4523 (1994).

24. D. C. Green, *J. Org. Chem.*, **44**, 1476 (1979).

25. E. F. Ullman, J. H. Osiecki, D. G. B. Boocock, R. Darcy, *J. Am. Chem. Soc.* **94**, 7049 (1972).

26. T. N. Baker, W. P. Doherty, W. S. Kelley, W. Newmeyer, J. E. Rogers, R. E. Spalding, R. I. Walter, *J. Org. Chem.*, **30**, 3714 (1965).

27. J. Berthelot, C. Guette, P. L. Desbène, J. J. Basselier, P. Cjaquin, D. Masure, *Can. J. Chem.*, **67**, 2061 (1989).

28. D. G. Boocock, R. Darcy, E. F. Ullman, *J. Am. Chem. Soc.* **90**, 5945 (1968).

29. F. Wudl, G. M. Smith, E. J. Hufnagel., *J. Chem. Soc. Chem. Commun.*, **1970**, 1453.

30. W. T. Borden, E. R. Davidson, *J. Am. Chem. Soc.*, **99**, 4587 (1977).

31. MOPAC Ver. 6.00 (QCPE No. 445), Stewart, J. J. *QCPE Bull.* **10(4)**, 86 (1990).

32. K. Yamaguchi, M. Okumura, T. Fueno, K. Nakasuji, *Synthetic Metals* , **41-43**, 3631, (1991).

33. (a) P. Nachtigall, K. D. Jordan, *J. Am. Chem. Soc.*, **115**, 270 (1993).

34. (a) A. A. Ovchinnikov, *Theor. Chim. Acta*, **47**, 297 (1978). (b) H. C. Longuet-Higgins, *J. Chem. Phys.*, **18**, 265 (1950).

35. K. Yamaguchi, M. Okumura, T. Fueno, K. Nakasuji, *Synthetic Metals*, **41-43**, 3631 (1991).

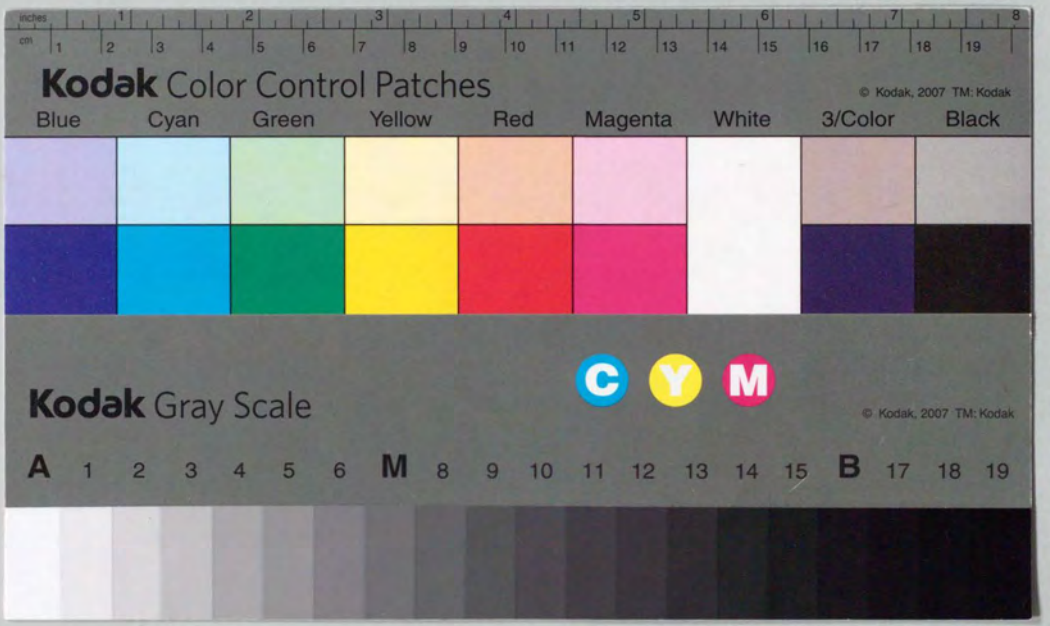
inches
cm
Kodak Color Control Patches
© Kodak, 2007 TM: Kodak
Blue
Cyan
Green
Yellow
Red
Magenta
White
3/Color
Black
Kodak Gray Scale
C
Y
M
© Kodak, 2007 TM: Kodak
A 1 2 3 4 5 6 M 8 9 10 11 12 13 14 15 B 17 18 19